SSC-341

GLOBAL ICE FORCES AND SHIP RESPONSE TO ICE

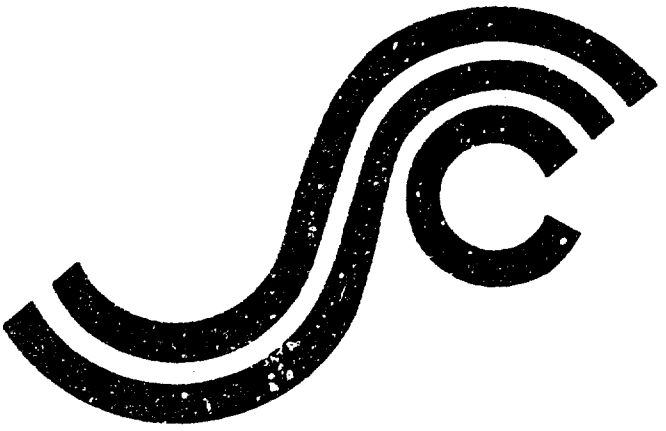

SHIP STRUCTURE COMMITTEE

1990

SHIP STRUCTURE COMMITTEE

The SHIP STRUCTURE COMMITTEE is constituted to prosecute a research program to improve the hull structures of ships and other marine structures by an extension of knowledge pertaining to design, materials, and methods of construction.

RADM J. D. Sipes, USCG, (Chairman)
Chief, Office of Marine Safety, Security and Environmental Protection
U. S. Coast Guard

Mr. Alexander Malakhoff
Director, Structural Integrity Subgroup (SEA 55Y)
Naval Sea Systems Command

Dr. Donald Liu
Senior Vice President
American Bureau of Shipping

Mr. H. T. Haller
Associate Administrator for Ship-building and Ship Operations
Maritime Administration

Mr. Thomas W. Allen
Engineering Officer (N7)
Military Sealift Command

CDR Michael K. Parmelee, USCG,
Secretary, Ship Structure Committee
U. S. Coast Guard

CONTRACTING OFFICER TECHNICAL REPRESENTATIVES

Mr. William J. Siekierka
SEA 55Y3
Naval Sea Systems Command

Mr. Greg D. Woods
SEA 55Y3
Naval Sea Systems Command

SHIP STRUCTURE SUBCOMMITTEE

The SHIP STRUCTURE SUBCOMMITTEE acts for the Ship Structure Committee on technical matters by providing technical coordination for determinating the goals and objectives of the program and by evaluating and interpreting the results in terms of structural design, construction, and operation.

AMERICAN BUREAU OF SHIPPING

Mr. Stephen G. Arntson (Chairman)
Mr. John F. Conlon
Mr. William Hanzalek
Mr. Philip G. Rynn

MILITARY SEALIFT COMMAND

Mr. Albert J. Attermeyer
Mr. Michael W. Touma
Mr. Jeffery E. Beach

MARITIME ADMINISTRATION

Mr. Frederick Seibold
Mr. Norman O. Hammer
Mr. Chao H. Lin
Dr. Walter M. Maclean

NAVAL SEA SYSTEMS COMMAND

Mr. Robert A. Sielski
Mr. Charles L. Null
Mr. W. Thomas Packard
Mr. Allen H. Engle

U. S. COAST GUARD

CAPT T. E. Thompson
CAPT Donald S. Jensen
CDR Mark E. Noll

SHIP STRUCTURE SUBCOMMITTEE LIAISON MEMBERS

U. S. COAST GUARD ACADEMY

LT Bruce Mustain

U. S. MERCHANT MARINE ACADEMY

Dr. C. B. Kim

U. S. NAVAL ACADEMY

Dr. Ramswar Bhattacharyya

STATE UNIVERSITY OF NEW YORK MARITIME COLLEGE

Dr. W. R. Porter

WELDING RESEARCH COUNCIL

Dr. Martin Prager

NATIONAL ACADEMY OF SCIENCES - MARINE BOARD

Mr. Alexander B. Stavovy

NATIONAL ACADEMY OF SCIENCES - COMMITTEE ON MARINE STRUCTURES

Mr. Stanley G. Stiansen

SOCIETY OF NAVAL ARCHITECTS AND MARINE ENGINEERS - HYDRODYNAMICS COMMITTEE

Dr. William Sandberg

AMERICAN IRON AND STEEL INSTITUTE

Mr. Alexander D. Wilson

Member Agencies:

United States Coast Guard
Naval Sea Systems Command
Maritime Administration
American Bureau of Shipping
Military Sealift Command

Ship Structure Committee

An Interagency Advisory Committee
Dedicated to the Improvement of Marine Structures

Address Correspondence to:

Secretary, Ship Structure Committee
U.S. Coast Guard (G-MTH)
2100 Second Street S.W.
Washington, D.C. 20593-0001
PH: (202) 267-0003
FAX: (202) 267-0025

SSC-341
SR-1313

December 3, 1990

GLOBAL ICE FORCES AND SHIP RESPONSE TO ICE

This report is the fourth in a series of six that address ice loads, ice forces, and ship response to ice. The data for these reports were obtained during deployments of the U.S. Coast Guard Icebreaker POLAR SEA. This report describes the method used to determine global ice impact forces from strain gage measurements and includes hull girder stress calculations and impact force time histories. The other ice reports are published as SSC-329, SSC-339, SSC-340, SSC-342 and SSC-343.

J. D. SIPES
Rear Admiral, U.S. Coast Guard
Chairman, Ship Structure Committee

Technical Report Documentation Page

1. Report No.	2. Government Accession No.	3. Recipient's Catalog No.
SSC-341		

4. Title and Subtitle	5. Report Date
Global Ice Forces and Ship Response to Ice	August 1990
	6. Performing Organization Code

7. Author(s)	8. Performing Organization Report No.
P. Minnick, J. St John, B. Cowper, M. Edgecombe	AEI 1092C/1095C ACL 1923A-DFR

9. Performing Organization Name and Address		10. Work Unit No. (TRAIS)
ARCTEC Engineering,Inc. 9104 Red Branch Road Columbia, MD 21045 USA	ARCTEC Canada Limited 16-6325 11th St., SE Calgary, Alberta Canada T2H 2L6	11. Contract or Grant No.

12. Sponsoring Agency Name and Address		13. Type of Report and Period Covered
Maritime Administration U.S.Dept. of Trans 400 Seventh Street, SW Washington, D.C. 20593	Transport Development Ctr. 200 Dorchester Blvd.,West Suite 601, West Tower Montreal, Quebec Canada H2Z 1X4	Final Report 14. Sponsoring Agency Code MAR-760

15. Supplementary Notes This was an international joint project between the Ship Structure Committee (USA) and the Transport Development Centre (Canada). The U.S. Maritime Administration served as the sponsoring agency for the interagency Ship Structure Committee.

16. Abstract During September and October of 1985 the Polar Sea conducted ice impact tests on heavily ridged ice features in the Alaskan portion of the Beaufort Sea. Bending strain gage measurements were used to estimate the longitudinal bending moment distribution of the POLAR SEA during impacts with ice pressure ridges. Compressive strains along the stem and ship acceleration and velocity measurements were also recorded. This paper describes the methodology for determining the global ice impact force from the measurements and presents the results of these tests. A comparison of the results with other available data is also presented. Hull strain, and impact force time histories are presented along with the longitudinal bending and shear distributions during ice impact events. The results indicate that the methodology used in estimating the impact force provided and excellent understanding of ship-ice interaction.

17. Key Words	18. Distribution Statement
Design Criteria Ice Loads Icebreakers Shipboard Loads Measurement	Document is available to the U.S. Public through the National Technical Information Service, Springfield, VA 22161

19. Security Classif. (of this report)	20. Security Classif. (of this page)	21. No. of Pages	22. Price
Unclassified	Unclassified		

Form DOT F 1700.7 (8-72) Reproduction of completed page authorized

METRIC CONVERSION FACTORS

Approximate Conversions to Metric Measures

Symbol	When You Know	Multiply by	To Find	Symbol
LENGTH				
in	inches	*2.5	centimeters	cm
ft	feet	30	centimeters	cm
yd	yards	0.9	meters	m
mi	miles	1.6	kilometers	km
AREA				
in^2	square inches	6.5	square centimeters	cm^2
ft^2	square feet	0.09	square meters	m^2
yd^2	square yards	0.8	square meters	m^2
mi^2	square miles	2.6	square kilometers	km^2
	acres	0.4	hectares	ha
MASS (weight)				
oz	ounces	28	grams	g
lb	pounds	0.45	kilograms	kg
	short tons (2000 lb)	0.9	tonnes	t
VOLUME				
tsp	teaspoons	5	milliliters	ml
Tbsp	tablespoons	15	milliliters	ml
fl oz	fluid ounces	30	milliliters	ml
c	cups	0.24	liters	l
pt	pints	0.47	liters	l
qt	quarts	0.95	liters	l
gal	gallons	3.8	liters	l
ft^3	cubic feet	0.03	cubic meters	m^3
yd^3	cubic yards	0.76	cubic meters	m^3
TEMPERATURE (exact)				
°F	Fahrenheit temperature	5/9 (after subtracting 32)	Celsius temperature	°C

*1 in. = 2.54 cm (exactly). For other exact conversions and more detail tables see NBS Misc. Publ. 286, Units of Weight and Measures. Price $2.25 SD Catalog No. C13 10 286.

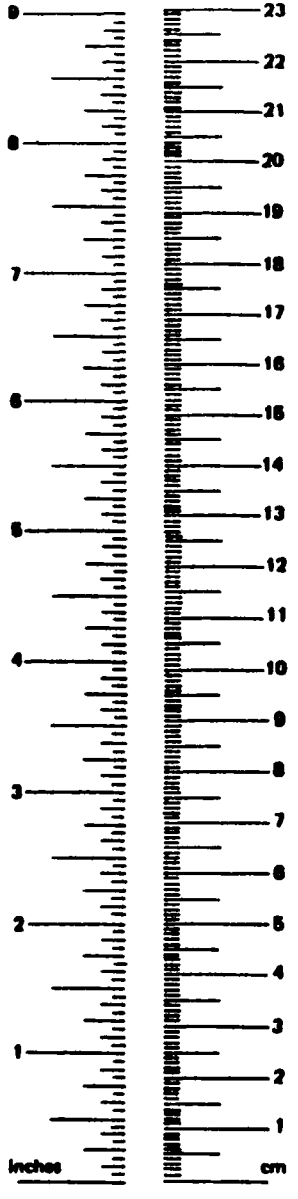

Approximate Conversions from Metric Measures

Symbol	When You Know	Multiply by	To Find	Symbol
LENGTH				
mm	millimeters	0.04	inches	in
cm	centimeters	0.4	inches	in
m	meters	3.3	feet	ft
m	meters	1.1	yards	yd
km	kilometers	0.6	miles	mi
AREA				
cm^2	square centimeters	0.16	square inches	in^2
m^2	square meters	1.2	square yards	yd^2
km^2	square kilometers	0.4	square miles	mi^2
ha	hectares (10,000 m^2)	2.5	acres	
MASS (weight)				
g	grams	0.035	ounces	oz
kg	kilograms	2.2	pounds	lb
t	tonnes (1000 kg)	1.1	short tons	
VOLUME				
ml	milliliters	0.03	fluid ounces	fl oz
l	liters	2.1	pints	pt
l	liters	1.06	quarts	qt
l	liters	0.26	gallons	gal
m^3	cubic meters	36	cubic feet	ft^3
m^3	cubic meters	1.3	cubic yards	yd^3
TEMPERATURE (exact)				
°C	Celsius temperature	9/5 (then add 32)	Fahrenheit temperature	°F

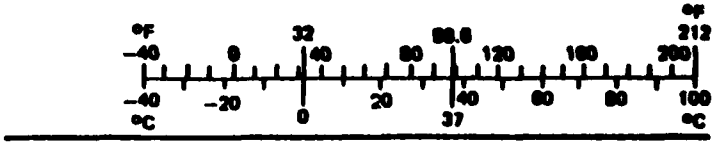

PREFACE

The overall objective of the project was to measure and analyze the global ice-hull interaction forces of a ship ramming in multi-year ice. Specific objectives were to obtain a larger data base of ice loads for the development of analytical models describing ship-ice interaction and analyze the effect of ship displacement and bow shape on global ice loads using the Canadian experience gained from the 1983 KIGORIAK and ROBERT LEMEUR Impact Tests [13].

An instrumentation system was developed for measurement of global ice impact loads onboard the USCGC POLAR SEA. From September 29, 1985, to October 12, 1985, the POLAR SEA conducted ice impact tests on heavily ridged ice features in the Alaskan portion of the Beaufort Sea. Bending strain gage measurements were used to estimate the longitudinal bending moment distribution of the POLAR SEA during an impact with an ice pressure ridge. Compressive strains along the stem and ship acceleration and velocity measurements were also recorded. Hull stress and impact force time-histories were calculated along with the longitudinal bending and shear distributions during ice impact events. The results indicated that the methodology used in estimating the impact force provided a greater understanding of the ship-ice interaction process.

One of the main conclusions from this study was that the ice force on the bow of the POLAR SEA should not be treated as a localized load. The load is spread over a large area of the bow from the stem hook forward. The longitudinal location of the maximum bending stress was just forward of the super-structure. The dominant response of the vessel was first mode vibration at about 3 Hz. The loading rate was measured to be as high as 5000 LT/sec (50 MN/sec), which is much lower than the 15,000 LT/sec (150 MN/sec) loading rate noted on the KIGORIAK [13]. The maximum vertical bow force observed during ramming was 2506 LT (24.97 MN) with a maximum measured bending stress of 6,078 psi (41.91 MPa). This is well below the 45,600 psi (310 MPa) yield strength for the hull material.

It is recommended that further analysis be done to determine the shape of the pressure distribution during each impact and to estimate the transverse force from unsymmetric rams. Both can be determined by additional analysis of the measured data. It is further recommended that additional multiyear ice data be collected with the POLAR Class. Additional data is required to better understand the relationship between vertical bow force and impact velocity.

TABLE OF CONTENTS

LIST OF FIGURES

LIST OF TABLES

1. INTRODUCTION

The USCG POLAR Class winter deployments sponsored by the Maritime Administration (MarAd) have provided a platform from which to gather environmental, trafficability, and ship performance data. For this phase of the program, a deployment of the POLAR SEA in September and October of 1985, the Ship Structure Committee, the American Bureau of Shipping and the Maritime Administration in conjunction with the Canadian Ministry of Transport sponsored a program to collect global ice loads. Additional support for this program as well as the concurrent environment data collection program was provided by Newport News Shipbuilding, Bethlehem Steel and five members of the Alaskan Oil and Gas Association (AOGA), Arco, Chevron, Exxon, Mobil and Shell.

The ultimate objective of this jointly funded research is to develop ice load criteria for the future design of ships. Specifically, the objective of this study was to measure the total load that ice exerts on the hull of the vessel when it rams large ice features. Other objectives included increasing the data base of ice loads for the development of analytical models describing the ship-ice interaction and for understanding the effect of ship displacement and bow shape upon the global ice loads by comparison with other available data.

The "global ice load" is defined as the net resultant of the ice loads generated at the many local contact areas around the bow during impact. These loads may generate significant bending moments in the hull girder, which may affect the structural integrity of icebreaking ships. This in turn has implications on the design of icebreaking vessels and the type of design criteria to be developed [1].

Since the start of commercial oil development in the Arctic a number of analytical models describing ship-ice interaction have been developed using a rigid body idealization, flexible beam elements, and three dimensional finite element models [2,3,4,5]. Full-scale impact tests have also been conducted on the icebreaking vessels M.V. CANMAR KIGORIAK [6,7], M.V. ROBERT LEMEUR [7,9], M.V. ARCTIC [10] and now the USCGC POLAR SEA. General discussions of these tests can be found in references 8 and 11. Physical modelling of the ship-ice impact interaction for the M.V. ARCTIC has also been carried out by ARCTEC CANADA for the Canadian Coast Guard [12] and the Technical Research Center of Finland under a joint research program. The focus of all the work has been to provide a sound technical basis for further development of ice load design criteria to accommodate the technical and regulatory requirements of expanding maritime operations in the Arctic.

The work presented here was carried out onboard the USCGC POLAR SEA in the Alaskan Beaufort Sea between September 19 and October 13, 1985. This report describes the way the global ice loads were collected as well as a presentation and analysis of the collected data. Figure 1 shows the principal areas of operation during the deployment.

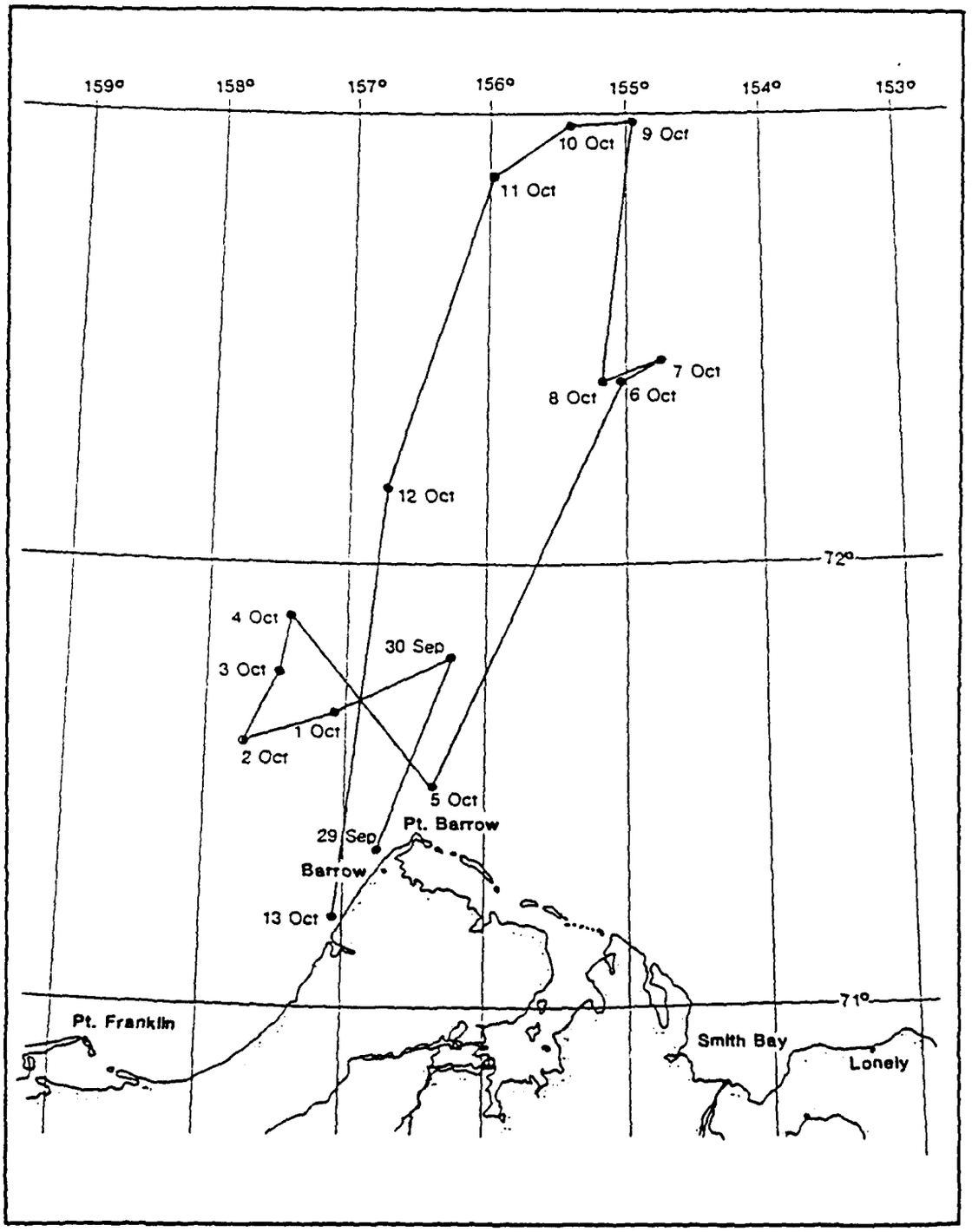

Figure 1
DAILY LOCATION OF POLAR SEA
AT 0000 LOCAL TIME

2. DESCRIPTION OF THE DATA ACQUISITION SYSTEM

An outline of the instrumentation system developed for this project is illustrated in Figure 2. The present system was adapted from the system originally developed by Canadian Marine Drilling Ltd. (Canmar) for the 1983 M.V. KIGORIAK and M.V. ROBERT LEMEUR full-scale impact tests [7]. There are several fundamental differences between these two systems. The approach used for Polar Sea measured the longitudinal bending strain distribution spanning the location of the ice load, whereas the Canmar system measured the shear strain in sections near the location of the ice load and the bending strain distribution aft of the location of the ice force. The POLAR SEA method required fewer strain gages at each location and therefore allowed more frames along the ship to be instrumented. The result was an excellent definition of the longitudinal bending and shear distribution spanning the location of the load because of the larger number of instrumented frames. Secondly, in these tests the actual longitudinal location of the load was measured from compressive strain gages along the centerline bulkhead, while the Canmar system had to infer the location from other data. Additional details of the POLAR SEA system as well as an itemized channel description are presented in Appendix A.

To estimate the vertical ice force on the bow during an impact with a heavy ice feature, the shear force around the location of the load must be well defined. Figure 3 gives some idealized shear and bending moment diagrams for an icebreaker ramming into an ice feature. As the lower figure indicates, the shear force changes from negative to positive over a relatively short distance around the location of the load. Since the shear force is the negative of the slope of the bending moment diagram, then the bending moment must be well defined over this same region in order to obtain an accurate estimate of the shear force. With this in mind, the majority of the frames instrumented for bending were concentrated near the anticipated location of the ice force. Figure 4 shows the location of these gages.

The bending gages along the O1 Deck and on the 3rd Deck at frame 55 were placed parallel to the side shell in pairs along opposite sides of the ship. Measurements taken from these gages were later transformed into the strain parallel to the centerline. (See Appendix B for the details involved in any of these conversions and computations.) In the calculation of the longitudinal strain due to the ice force, the data from each pair were averaged together to exclude any torsional strain. Another advantage of this gage pair arrangement was the ability to observe the symmetry, or the lack thereof, in the ice loading during a ram.

The bending gages were placed on at least two levels for every location forward of frame 86. This arrangement allowed the computation of the bending moment based upon a stress couple that was a known distance apart. It had the further advantage of eliminating the longitudinal stress, and therefore force, from the bending moment calculation.

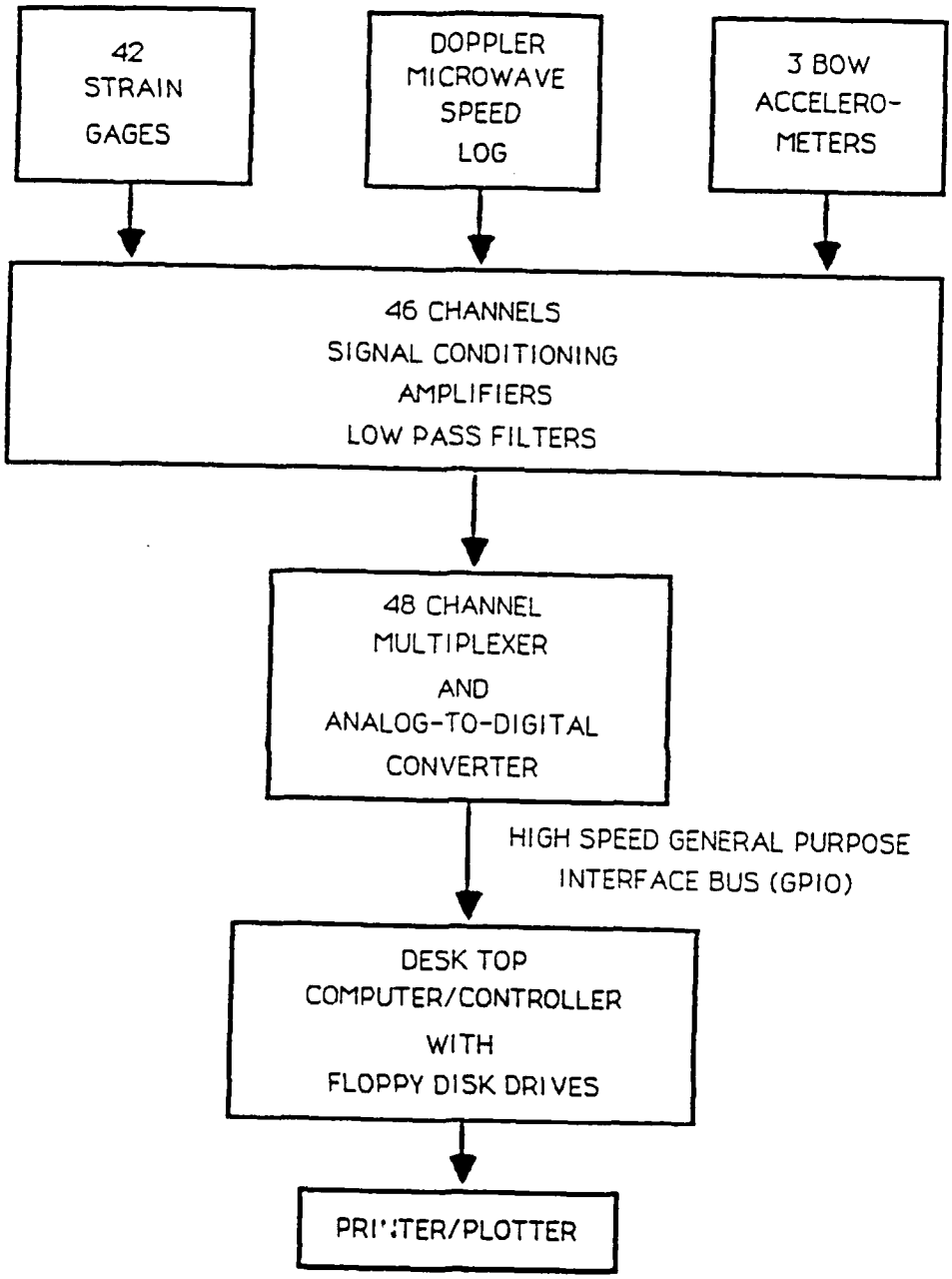

Figure 2

SCHEMATIC DIAGRAM OF THE GLOBAL LOADS DATA ACQUISITION SYSTEM

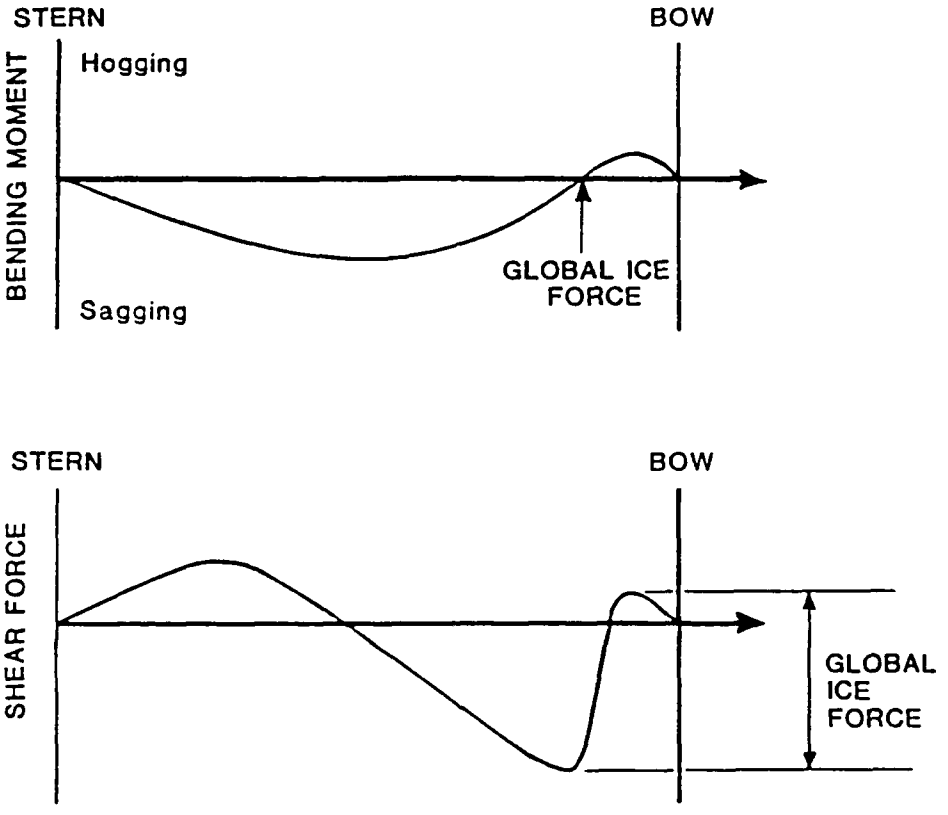

Figure 3

ESTIMATED SHEAR AND BENDING MOMENT DIAGRAMS FOR THE USCGC POLAR SEA

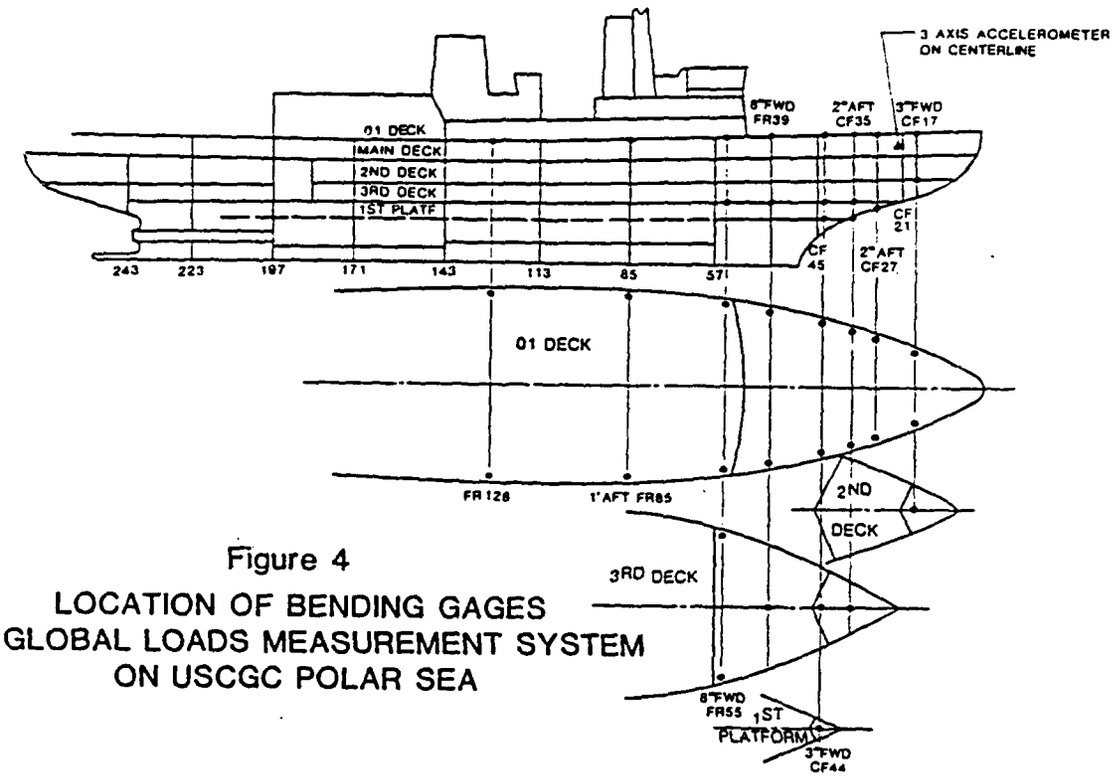

Figure 4

LOCATION OF BENDING GAGES
FOR GLOBAL LOADS MEASUREMENT SYSTEM
ON USCGC POLAR SEA

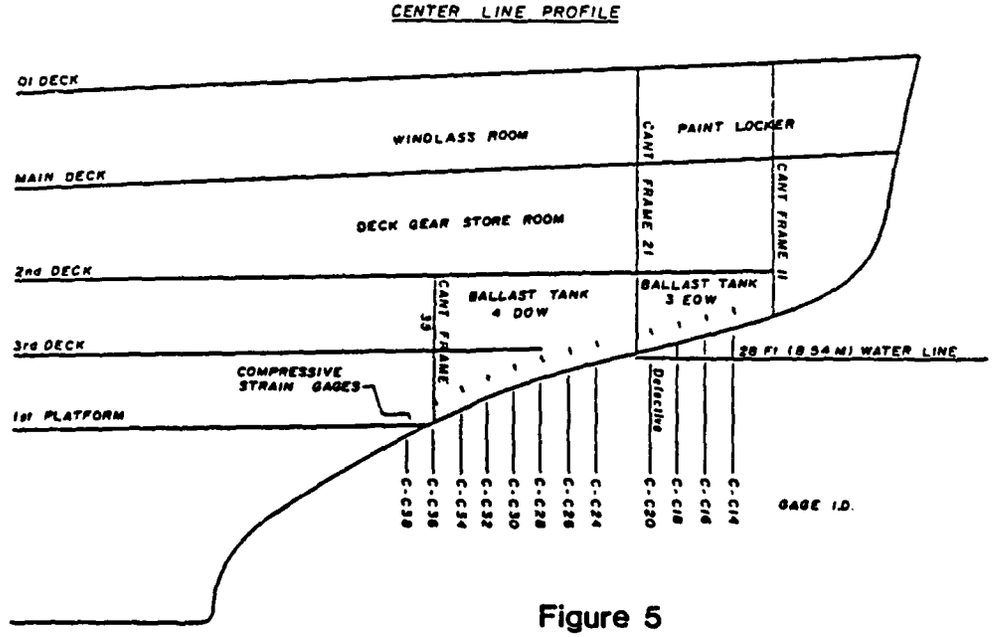

Figure 5

LOCATION OF LONGITUDINAL COMPRESSION GAGES

Compression gages for estimating the location of the load were installed from cant frame 14 to cant frame 38. They were placed on the centerline bulkhead, just forward of the cant frames and 12 to 18 inches above and perpendicular to the stem bar. Figure 5 shows these locations. The spacing of these gages enabled an accurate estimate of the center of the ice force to be made since the load could be "sensed" every 32 in (80cm) along the stem. The gage distance away from the stem bar was selected from work done on the placement of gages for measurement of local loads [15] to avoid the possibility of "dead spots" between the gages. This system also provided an estimate of the impact speed as the peak ice force moved along the stem bar.

Transverse compression gages were installed at cant frame 35 as shown in Figure 6. The output from these gages was intended for use in estimating the width of the ice contact area and the distribution of pressure across the bow of the POLAR SEA. These gages were added knowing that the analysis of the data could not be completed within the intitial scope of work. It is hoped that this data can be reduced in the future.

In addition to the strain gages, three uniaxial accelerometers arranged in a triaxial array and oriented to the ship's principal axes were located in the bow area as shown in Figure 4. The output from the yaw accelerometer was used to determine if a ram was symmetric. The accelerometer readings could also be used in future analysis to provide an estimate of the inertial forces forward of the ice force and help assess the relative importance of the longitudinal, transverse and vertical ice forces acting on the vessel. The POLAR SEA was also equipped with a doppler microwave speed log. This radar was mounted in the waist of the vessel and oriented forward to provide an estimate of the impact velocity. The specifications and locations of all the transducers used for the onboard instrumentation are described in Appendix A.

The required sampling frequency for measurement of the strain response of the POLAR SEA was selected based on the rate of loading and the vibrational frequency of the ship. Previous experiments have indicated that the dominant vibrational frequency was approximately 3 Hz [16]. The predicted rise time of the ice force was used to estimate the rate of loading. In this case, previous full-scale measurements indicated rise times to be as fast as 0.1 seconds [17]. If a quarter sine wave is assumed for the rise in strain, a corresponding maximum frequency of interest of 2.5 Hz results (period of 0.4 seconds). A low-pass filter frequency of 10 Hz was selected such that it was well above all the frequencies of interest. The minimum digital sampling frequency would then be 32 Hz to ensure a unique 10 Hz sine wave. This is exactly the system that was used in the local loads measurement program [15]. In this case a more sophisticated data acquisition system allowed an increase in sampling frequency over the local loads system, so 100 Hz was selected to provide at least 10 samples during the strain rise time. Data was sampled for 25 seconds which was determined by the size of the storage medium. To increase sampling frequency beyond 100 Hz, the length of recording would have to be shorter or a larger storage medium could be used. The chosen values were a reasonable compromise for the intended measurements.

LOCATION	CHANNEL I.D.
10S	C-C35-10S
11S	C-C34-11S
11P	C-C35-11P
10P	C-C35-10P
9P	C-C35-9P

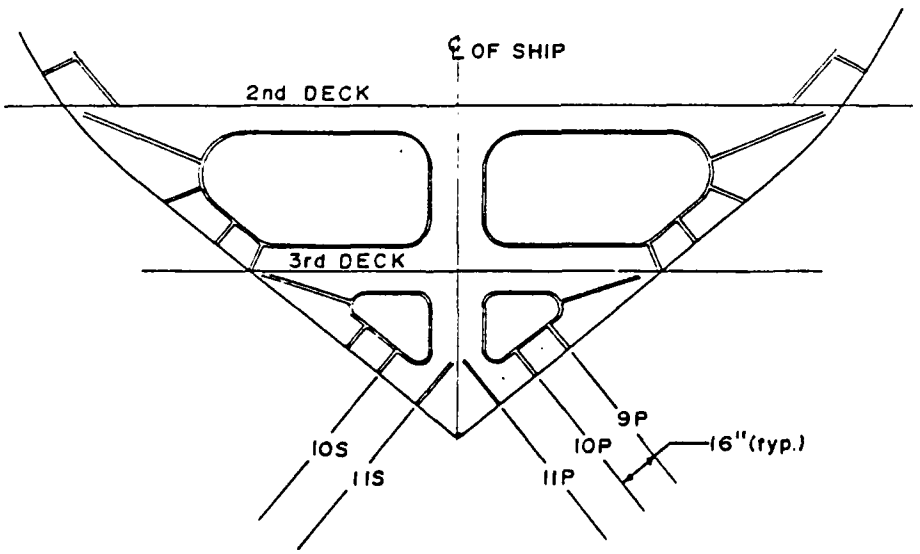

Figure 6

LOCATION OF TRANSVERSE COMPRESSION GAGES ON CANT FRAME 35

3. DESCRIPTION OF THE TEST PROGRAM

Global load data were gathered on the summer deployment of POLAR SEA to the Beaufort Sea. The program was completed in conjunction with an environmental data collection effort involving extensive on-ice surveying of surface and sub-surface topography. Measurement techniques included a surveyor's "total station" with electronic data logging for surface locations and elevations. A remotely operated vehicle with an upward-looking sonar, a Mesotech profiling sonar, and a thermal drill were used for thickness and sub-surface details. Table 1 gives a summary of the data collected at the seven sites documented during the deployment. A detailed description of the measured data as well as a description of the measurement techniques can be found in reference 18.

On Sunday, September 29,1985, the participants for the first (one week) leg of the program arrived onboard the USCGC POLAR SEA off Barrow, Alaska. The POLAR SEA proceeded approximately 40 nautical miles to the north to Site 1 and Site 2 (71.41 N, 157.03 W). The following two days were spent preparing the loads data acquisition system for operation and conducting on-ice measurements. Ice conditions in the area were composed of large first year ice floes with imbedded multiyear fragments. The heaviest parts of the floes ranged from 5 to 8 meters in thickness. A total of eight trial rams were conducted in the thinner parts of these floes to verify the correct operation of the data collection system during the evening of October 2. This was followed by two ramming tests against the heaviest ridge sections. These rams completely destroyed both of the principal features that had been profiled.

On October 2, a helicopter reconnaissance flight located another floe several miles away that contained thicker and more extensive multiyear ridges (Site 3 and Site 4: 71.54 N, 157.22 W). Ice profiling was conducted on October 3 and October 4. The principal multiyear ridge in this floe was found to have a keel of approximately 42 ft (13 m). On the evening of October 4, this ridge and several adjacent features were repeatedly rammed at speeds up to nine knots. A total of nine rams were obtained before all the thick sections of ice were substantially destroyed.

A personnel transfer was conducted off Barrow on October 5. Polar Sea proceeded approximately 60 nautical miles to the north to begin the second (eight day) leg of the global loads program. A helicopter reconnaissance was conducted while the ship was underway and Site 5 (72.23 N, 155.04 W) was located. Ice in the vicinity was a mixture of first to second year with some small multi-year fragments. Site 5 had a ridge with a maximum thickness of approximately 46 ft (14 m). Two ramming tests were performed on October 6 at the ice edge, however, only one of these tests was recorded. A total of three rams were conducted on the ridge, on October 8, each one breaking the ridge at various locations. Three more rams were conducted at surrounding thick ice features.

SITE	LOCATION LATITUDE/ LONGITUDE	SIZE OF SURVEY AREA	# OF SURVEY POINTS	MAX SAIL HEIGHT	MAX KEEL DEPTH	# OF SONAR HOLES
1	71°41'NW 157°03'W	290'X290'	172	13.5	36.1	3
2	71°41'N 157°03'W	210'x270'	140	10.5	28'	0
3	71°54'N 157°22'W	185'x215'	160	10.45	30.1	2
4	71°54'N 157°22'W	450'x360'	111	14.4	42.1	2
5	72°23'N 155°04'W	440'x270'	185	10.3	35.7	4
6	72°26'W 154°56'W	300'x200'	79	17.1	37.5	2
7	73°N 154°56'W	690'x310'	140	13.7	44.2	3

SITE	# OF THERMAL DRILL HOLES	TOTAL DEPTH OF THERMAL DRILL HOLES	ROV	# OF CORES	TOTAL CORE LENGTH	K/S
1	25	470'		0	0	2.67
2	71	1074'		2	158"	2.67
3	62	970'		1	174"	2.88
4	78	1630'	yes	2	336"	2.92
5	100	2161'	yes	3	429"	3.47
6	11	219'	yes	2	90"	2.19
7	0	0'	yes	2	78"	3.23

Table 1

SUMMARY OF PROFILED ENVIRONMENTAL CONDITIONS

On the night of October 8, a large ridge at Site 7 (73.00 N, 154.56 W) was found. In the following two days, the ridge was surveyed and found to have a maximum thickness of approximately 58 ft (18 m). The floe had melt ponds throughout and was composed of first and second year ice. A total of four rams were conducted on the ridge on October 10 each one breaking the ridge at the point of impact. Fourteen more rams, for a total of forty, were conducted on ridged ice features during the transit back to Barrow, Alaska, from October 11 to October 12.

In general, the typical operation was to locate an ice feature, position the ship in the floe next to the feature while surveying operations were conducted, and then to ram the measured feature to collect the ice loading data before moving on to the next site.

It was anticipated that more than forty ice impacts would be recorded during the deployment, but ice conditions were not as severe as expected. Ideal ice conditions for the tests would have been a large, thick multiyear floe that could be rammed repeatedly without breaking apart. Multiyear ice was only encountered in small floes (some with a reasonable size ridge that was surveyed) that were imbedded in first year ice. Much of the old ice was only second year. Table 2 summarizes the general characteristics of each ramming event.

A typical ramming test consisted of the following sequence of events. The icebreaker cleared a path to ram the ice feature. The vessel was moved perpendicular to the ridge feature and several ship lengths away before accelerating towards the ridge. Approximately five seconds prior to impact the data acquisition was started and data acquired for 25 seconds. Data collection was triggered by an operator viewing a video display of the bow of the vessel and the immediate area ahead of the ship. The measured data were transferred to a floppy disk that took approximately 60 seconds to store. When time permitted between ramming tests, the data were analyzed and plotted.

TABLE 2

OBSERVATIONS OF RAMMING TESTS

Ram No.	Date	Symmetric	Magnitude of Measured Load*	Description of Ice Feature	Comments**
1	10/02	Y	L	Site 1	
2	10/02	Y	L	Site 2	Good Hit
3	10/04	Y	L	Site 3	12 m Ridge
4	10/04	Y	L	Site 3	
5	10/04	Port	L	Site 4	Good Heave
6	10/04	Port	S	Site 4	Roll & Pitch
7	10/04	Y	S	Small Floe	Good Acc. ch
8	10/04	Y	S	Small Floe	Floe Submerged
9	10/04	Y	S		
10	10/04	Y	S	Small Floe	
11	10/04	Y	S	Small Floe	
12	10/04				Not Recorded
13	10/06				
14	10/07	Y	S	Site 5	Beaching Force
15	10/07	Y	S	Site 5	
16	10/07	Y	L	Site 5	2nd Hit Hard
17	10/08	Y	L	Site 6	3 Hits
18	10/08	Y	L	Site 6	Hit Ice Knife
19	10/08	Stbd.	S	Site 6	Bounced to Port
20	10/08	Y	S	Small Floe	
21	10/08	Y	L	Small Ridge	
22	10/08	Y	L	Small Ridge	
23	10/08	Y	L	Cent. Site 7	3 Hinge Break
24	10/10	Y	L	Right Site 7	Floe Submerged
25	10/10	Y	VL	Left Site 7	Floe Submerged
26	10/10	Y	VL	Right Site 7	Floe Submerged
27	10/11	Y	S	In Transit	Small Ridge
28	10/11	Y	S	In Transit	Small Ridge
29	10/11	Y	S	In Transit	Small Ridge
30	10/11	Y	S	In Transit	Small Ridge, Ridge Not Broken
31	10/11	Y	M	In Transit	Small Ridge
32	10/11	Stbd.	M	In Transit	Glanced to Port
33	10/11	Y	M	In Transit	Large Heave
34	10/11	Y	VL	In Transit	Good Hit
35	10/11	Y	M	In Transit	
36	10/11	Y	S	In Transit	Light Hit
37	10/12	Y	S	In Transit	Beaching Force, Not Broken
38	10/12	Y	S	In Transit	Impact into previous bow print, second ram, feature not broken
39	10/12	Y	VL	In Transit	Good Impact, third ram, Ridge broken
40	10/12	Port	L	In Transit	Hit Port Side

* S, M, L, & VL indicates small, medium, large, and very large bow force loads.
** All rams resulted in failure of the ice feature except where noted.

4. ANALYSIS PROCEDURES AND RESULTS

The procedures used to analyze the data from each ramming event are summarized here. Appendix B gives a more detailed description and derivations of the various equations used.

The analysis software was separate from the data acquisition software. This allowed flexibility during the data collection process since several good rams could occur a few minutes apart. The separation of these functions (data acquisition and analysis) meant that the information could be collected and stored for future analysis without missing any opportunities to collect data during sequential rams.

The analysis software was derived from the program written for the KIGORIAK and ROBERT LEMEUR impact tests conducted in 1983. Its main function was to calculate and plot the vertical bow force time-history acting on the POLAR SEA, and determine the time of the maximum bow force together with the location along the stem. It was also used to graph the shear force and bending moment distributions at any time-step during the 25 second sampling interval. In addition to these functions, the analysis software performed a number of secondary calculations such as plotting the strain time-history from any of the gages, or finding the location of the neutral axis at frames instrumented on two separate levels. Appendix C contains a summary of the program's features and a flow chart showing the branching structure.

During the analysis, the deck bending strain time-history at each gage location is calculated and plotted for every ram. Zeros on all channels are determined by averaging the data obtained just prior to the impact and subtracting them from the subsequent measurements. Stresses are calculated by multiplying the results by a calibration factor and the elastic modulus. The gages that were placed parallel to the side shell of the vessel are multiplied by another transformation factor to arrive at the bending stress parallel to the centerline. Appendix A contains a listing of the gage calibration factors used, while Appendix B gives the derivation of the centerline stress transformation for each instrumented frame.

A sample plot of the bending stress at frame 39 (usually the location of the highest bending stress) is shown in Figure 7. During the ramming tests, the maximum bending stress was typically determined within a minute of completion of the ram. These values were always well below the yield stress of the 01 Deck which is 45,600 psi (310 MPa). A histogram of the maximum bending stress is given in Figure 8 which shows that the highest bending stress recorded is about 6500 psi (45 MPa).

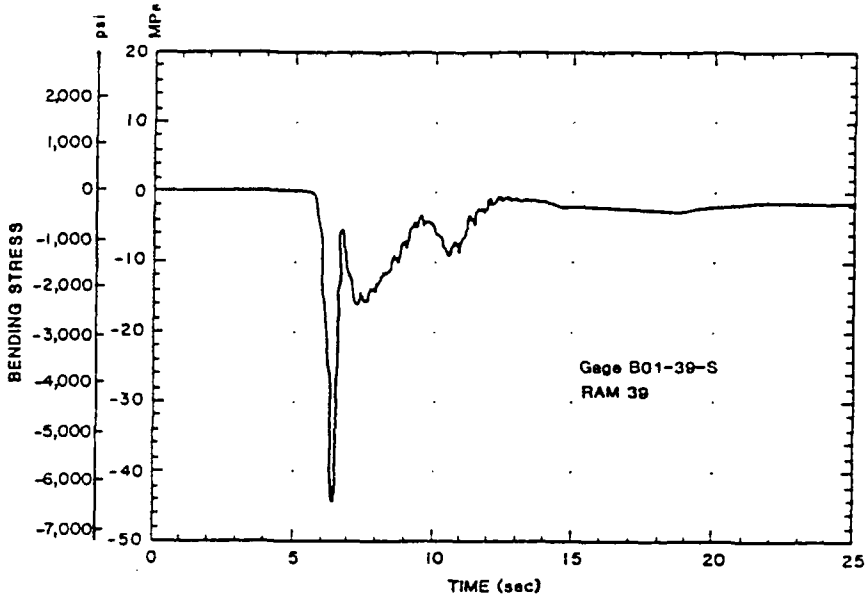

Figure 7
BENDING STRESS TIME HISTORY AT FRAME 39

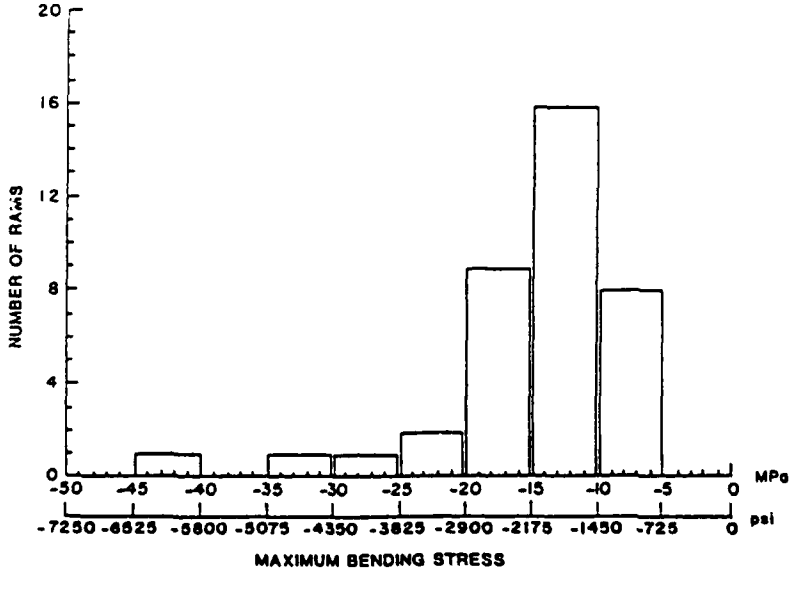

Figure 8
HISTOGRAM OF MAXIMUM BENDING STRESS

Figure 9 illustrates excitation of the first mode natural frequency of the hull girder. This figure shows the stress time-history measured by the starboard bending gage located at frame 128 near amidships on the 01 Deck. The measured frequency of 3.0 Hz is within 8% of a previously measured value of 2.75 Hz [2] and very close to the 2.9 Hz computed by the finite element model constructed by ABS.

In order to compute a bending moment from the bending stresses, it was assumed that when the USCGC POLAR SEA impacts a heavy ice feature it responds similar to a beam for bending within the centerline plane. The bending moment at each instrumented frame was then calculated using the bending stresses and structural properties of the vessel.

$$M = \frac{\sigma \cdot I}{Y}$$

where
- σ = Bending stress = $\varepsilon \cdot E$
- ε = Strain (parallel to the centerline)
- E = Elastic modulus
- I = Transverse sectional moment of inertia
- Y = Distance between gage and neutral axis or the distance between gage pairs on the same frame

Referring again to Figure 4 which gives the locations of the bending gages, it can be seen that several of the frames offer a couple of different methods for applying this formula. At cant frame 44, for instance, the stresses at the gages on the 01 Deck are averaged together and used in conjunction with either the gage on the Third Deck or the First Platform. Or, for that matter, the 01 Deck gages could be used alone along with their vertical distance from the neutral axis. Generally however, a gage "couple" was used except for the cases where bending gages were installed along the stem bar and a few of the other centerline gages. These particular gages were found to respond to the local load of the ice moving down the stem bar or other stress concentration influences and hence were not used in the calculations.

Once the bending moment distribution along the length of the ship was obtained, the shear force was computed as the negative slope (derivative) of the longitudinal bending moment curve. Figure 3 shows, generally, how these curves appeared.

Figure 3 also shows how the global ice force is related to the shear diagram. The force on the bow was calculated by the addition of the absolute value of the greatest shear force forward and aft of the load. The location of the center of the vertical ice load was estimated from the measurements received from the compression gages arranged along the stem bar. At any instant in time, the location of the compression gage with the largest compressive strain was taken as the ice load's location.

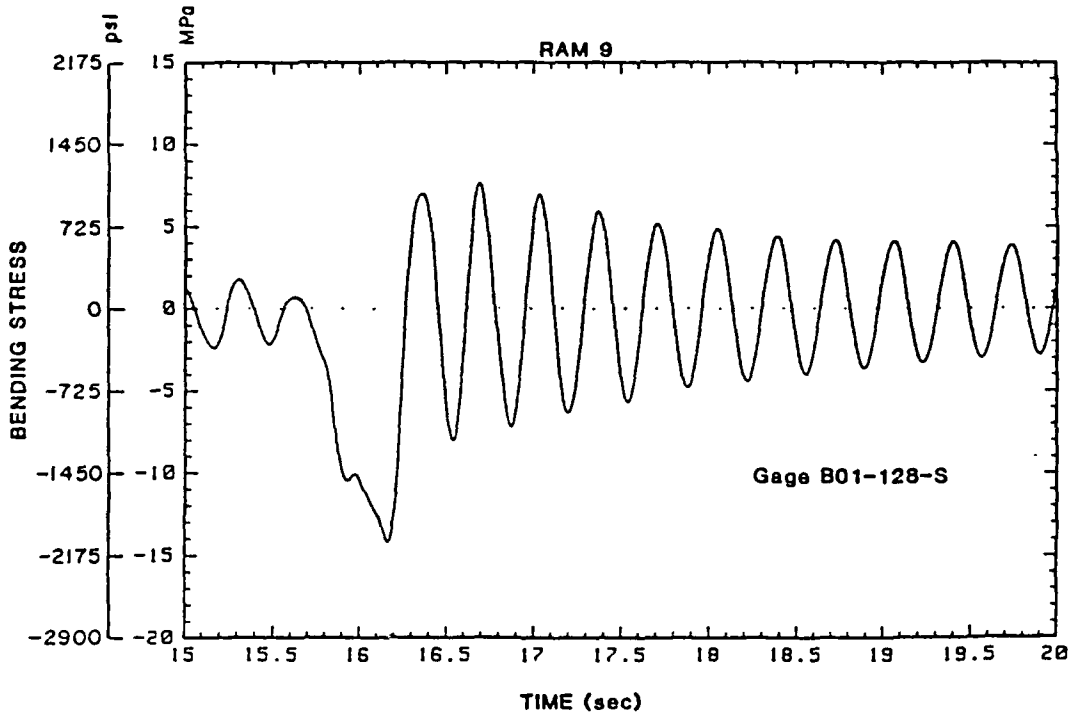

Figure 9

BENDING STRESS TIME HISTORY NEAR MIDSHIPS (FRAME 128)

This entire procedure was repeated for every time step (0.01 seconds) for the duration of the ramming test (25 seconds). The result of these computations was a time-history of the vertical bow force during the ramming event. Figure 10 gives a bow force time-history plot for one of the more severe impacts. Representative rams were analyzed onboard the vessel using preliminary estimates for the sectional inertias and locations of the neutral axes.

It was anticipated that if the ice load occurred forward of cant frame 17, then the shear force would be estimated by the multiplication of the measured vertical acceleration and the mass of the bow section forward of the load. The maximum value for this inertial force, however, was estimated to be approximately 30 LT (0.3 MN) which is less than the uncertainty expected in computing the vertical bow force and was therefore neglected (Section 6 discusses the error analysis).

The onboard data analysis indicated that while in the ramming mode the superstructure of the POLAR SEA contributed significantly to the flexural stiffness of the vessel. This was apparent when the calculated bending moment at frame 55 (using a section modulus which did not include the effect of the superstructure) was much less than that calculated at frame 39. As Figure 4 shows, frame 39 is just forward of the superstructure and only 20.6 ft (6.3 m) forward of frame 55. The bending moment distribution for this portion of the ship should have a relatively smooth shape.

The calculated bow force determined from the discontinuity in the shear curve was always located forward of the superstructure and hence unaffected by the sectional properties for the frames under the superstructure. Based on this observation, it was decided that "effective" sectional properties could be found for these frames for use in the final calculations. The location of the effective neutral axis was calculated at frames where the bending strain was measured at two levels by assuming a linear stress distribution through the cross-section. The point where this distribution passed through zero was taken to be the effective neutral axis. The moment of inertia for each of these cross-sections was recalculated from the ship's drawings based upon the new location for the neutral axis. With the assumption that the ship remains in a quasi-static equilibrium, the areas above and below the shear diagram were calculated to determine if they were equal. This was done as a check on the validity of the recalculated sectional properties since they were not equal using the original estimates. The sectional properties for the frames including the superstructure were then adjusted to bring the positive and negative areas of the shear graph into equilibrium.

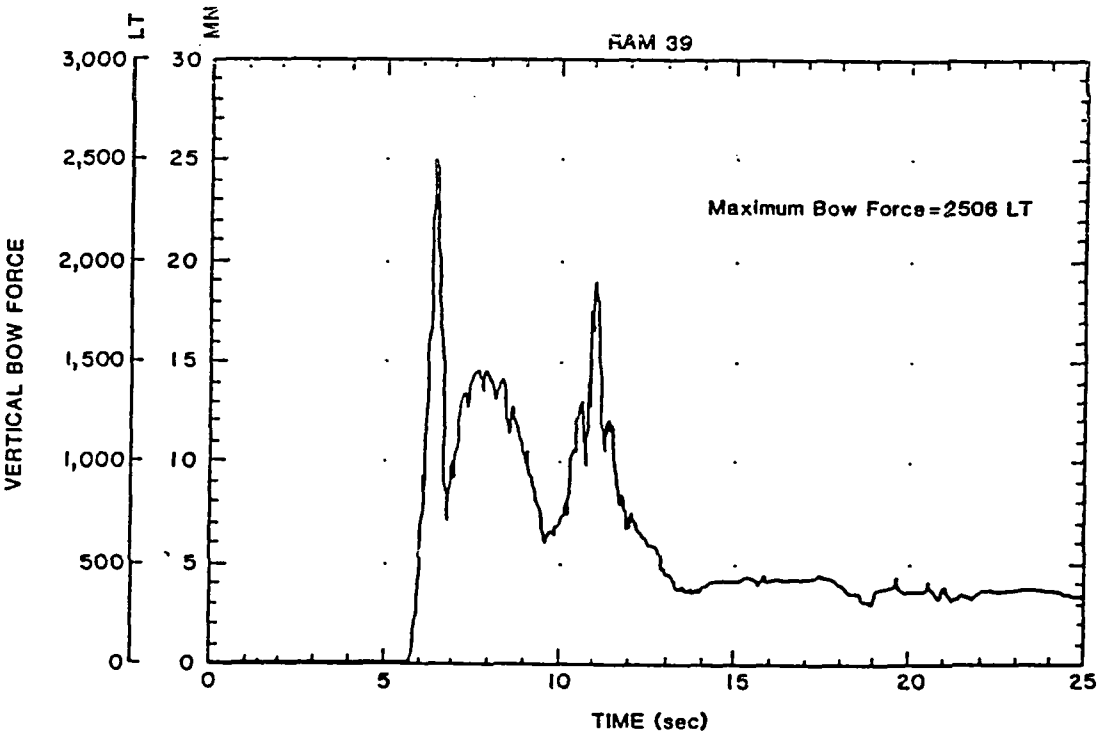

Figure 10
VERTICAL BOW FORCE TIME HISTORY

Table 3 below gives a listing of the revised neutral axes and moment of inertias for each of the instrumented frames on the POLAR SEA. These are the values used in the final calculations.

TABLE 3

SECTIONAL PROPERTIES FOR THE POLAR SEA (WAGB-11)

LOCATION	NEUTRAL AXIS ft (m)	MOMENT OF INERTIA $ft^4 (m^4)$
Frame 128	24.3 (7.41)	11,586 (100)
Frame 86	25.8 (7.86)	11,586 (100)
Frame 55	25.3 (7.7)	15,062 (130)
Frame 39	28.2 (8.6)	7,623.7 (65.8)
Cant Frame 44	34.8 (10.6)	3,058.8 (26.4)
Cant Frame 35	37.1 (11.3)	2,085.5 (18.0)
Cant Frame 27	40.4 (12.3)	1,181.8 (10.2)
Cant Frame 17	42.6 (13.0)	787.9 (6.8)

As a check on the validity of the algorithm used to calculate the total vertical ice force on the bow, a comparison was made with the beaching force computed from hydrostatics. A couple of representative rams were selected where the ship came to a complete stop. This insured that the longitudinal force would be negligible. At the instant of zero headway, the vertical bow force was computed using the measurements obtained from the bending gages.

At the same time the angle of trim, ϕ, was estimated from the accelerometer data. The hydrostatic curves were then used to obtain the moment to trim one inch (MTI) and the beaching force calculated from

$$F = \sin\phi \cdot LBP \cdot MTI / d$$

LBP = Length between perpendiculars

where d is the approximate distance from the point of application of the ice force to the longitudinal center of flotation. Appendix B contains further details of this calculation. Table 4 gives some of these results from which it can be seen that the values obtained using the different methods are in fairly good agreement.

TABLE 4

HYDROSTATIC AND CALCULATED BOW FORCE

RAM NO.	FORCE FROM HYDROSTATIC CURVES LT (MN)	FORCE CALCULATED FROM BENDING GAGES LT (MN)
37	542 (5.4)	572 (5.7)
39	371 (3.7)	361 (3.6)

The location of the center of the ice force (calculated from output of the stem bar compression gages) during ramming can be used to estimate the impact velocity. A sample plot of the calculated location of the load versus time is shown in Figure 11. The slope of a line drawn through this stepped curve is an estimate of the velocity of the ice movement along the stem bar. Correcting for the angle of the stem bar, an approximate value for the ship impact velocity is obtained. A comparison between the impact velocity calculated from the location of the load time-history and the velocity measured from the doppler speed log for two rams is shown in Table 5.

TABLE 5

COMPARISON OF IMPACT VELOCITIES

RAM NO.	DOPPLER SPEED LOG		STEM BAR GAGES	
	knots	(m/sec)	knots	(m/sec)
8	7.0	(3.6)	8.6	(4.4)
9	6.8	(3.5)	7.6	(3.9)

The difference in velocities is probably due to the nature of the ship-ice interaction. The ice moving down the stem bar is not exactly a point load and does experience some crushing causing the point of maximum loading to shift locations within the ice feature. In any event, the velocities given are relatively close.

All of the strain data was analyzed using the procedure described above. Table 6 summarizes the results for all of the rams and gives the peak vertical bow force, the impact velocity, and the maximum bending stress along the 01 Deck. The largest bow force encountered was 2506 LT (24.97 MN) during ram number 39. This ram also obtained the highest bending stress with 6078 psi (41.91 MPa) in compression at frame 39. A histogram of the peak vertical force is illustrated in Figure 12.

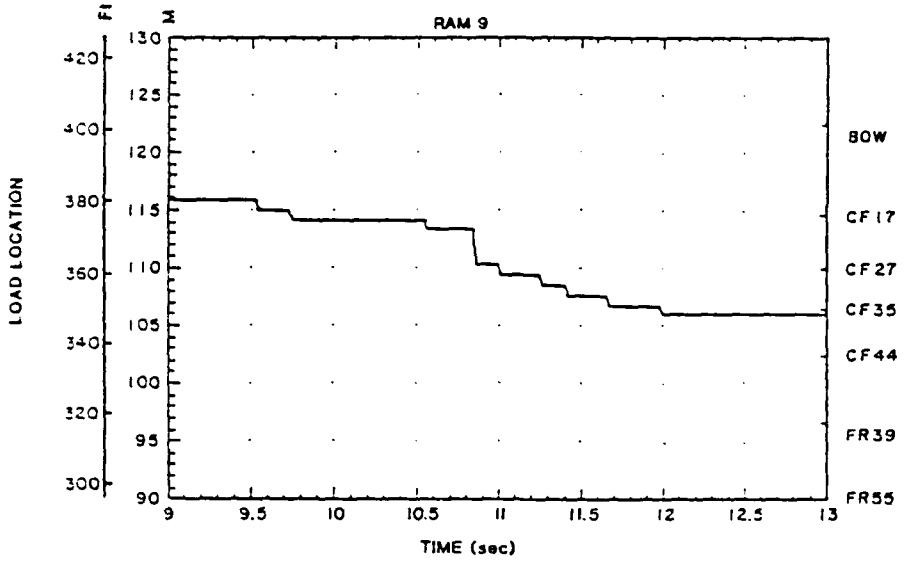

Figure 11

LOCATION OF THE LOAD FORWARD OF THE STERN vs. TIME

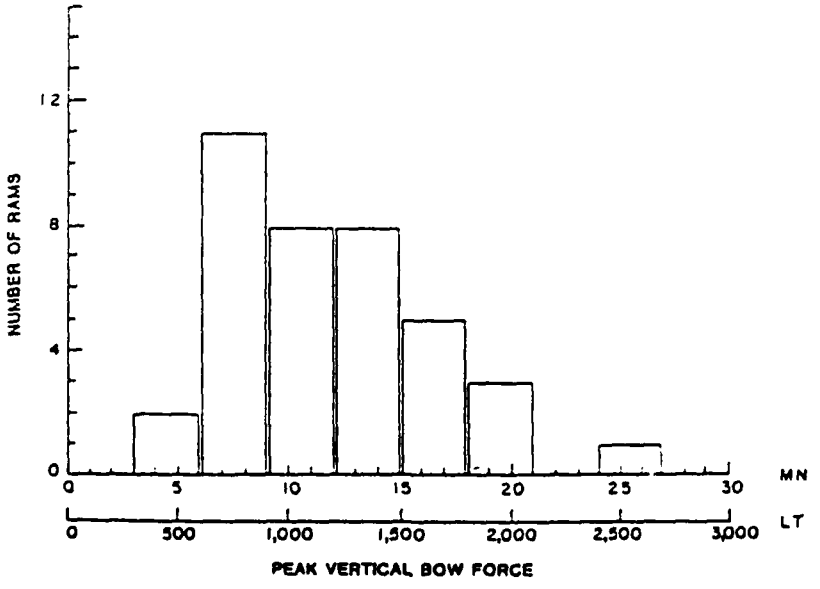

Figure 12

HISTOGRAM OF PEAK BOW FORCE

TABLE 6

SUMMARY OF IMPACT DATA ANALYSIS

RAM NUMBER	IMPACT VELOCITY		MAX. VERTICAL BOW FORCE		MAX. BEND. STRESS	
	kts	m/s	LT	MN	psi	MPa
1	8.3	4.3	851	8.48	-1530	-10.55
2	8.9	4.6	1672	16.66	-3545	-24.44
3	8.5	4.4	1516	15.11	-2515	-17.34
4	5.9	3.0	552	5.50	-1008	- 6.95
5	8.6	4.4	1402	13.97	-2235	-15.41
6	5.9	3.0	804	8.01	-1748	-12.05
7	6.1	3.1	1121	11.17	-1320	- 9.10
8	7.0	3.6	806	8.03	-2054	-14.16
9	7.0	3.6	1409	14.04	-3758	-25.91
10	7.0	3.6	679	6.77	-1498	-10.33
11	8.6	4.0	717	7.14	-1697	-11.70
13	4.0	2.1	528	5.26	-1043	- 7.19
14	4.3	2.2	1610	16.04	-2554	-17.61
15	5.7	2.6	1465	14.60	-1872	-12.91
17	8.5	4.4	1624	16.18	-1997	-13.77
18(1)	6.0	3.1	1473	14.68	-2312	-15.94
19	4.8	2.5	1291	12.86	-2196	-15.14
20	6.9	3.5	1151	11.47	-2055	-14.17
21	8.5	4.4	1204	12.36	-1814	-12.51
22(1)	6.0	3.1	1063	10.59	-1993	-13.74
23	8.8	4.5	991	9.87	-1510	-10.41
24(1)	7.0	3.6	841	8.38	-1523	-10.50
25	7.5	3.9	1959	19.52	-4364	-30.09
26	9.0	4.6	1463	14.58	-2716	-18.73
27(1)	6.0	3.1	768	7.65	-1411	- 9.73
28(2)	x		919	9.16	-1516	-10.45
29(2)	x		613	6.11	-1357	- 9.36
30(2)	x		688	6.86	-1389	- 9.58
31	5.0	2.6	1101	10.97	-1682	-11.60
32	5.0	2.6	1009	10.05	-1524	-10.51
33	11.5	5.9	2051	20.44	-2828	-19.50
34	10.9	5.6	1418	14.13	-2445	-16.86
35	6.6	3.4	679	6.77	-1352	- 9.32
36(1)	9.0	4.6	934	9.31	-1846	-12.73
37	6.0	3.1	650	6.48	-1433	- 9.88
38	6.2	3.2	1923	19.16	-2483	-17.12
39	8.5	4.4	2506	24.97	-6078	-41.91
40	7.6	3.9	1603	15.97	-3192	-22.01

(1) Data from bridge velocity indicator
(2) Data not available

5. COMPARISON OF POLAR SEA RESULTS WITH PREVIOUS REPORTS

5.1 Peak Vertical Bow Force Versus Impact Velocity

The results obtained from the full-scale impact tests onboard the USCGC POLAR SEA can be compared with previous predictions of vertical bow force on icebreaking vessels. Figure 13 gives a scatter plot of the vertical bow force versus the impact velocity for all impact events. Added to this plot are several maximum vertical bow force prediction curves. The solid curve comes from a proposal by Johansson, Keinonen, and Mercer [14] for Arctic Class 10 vessels. They felt that the total maximum bow force was largely influenced by the ship's speed and mass and gave a recommended design equation of

$$F_{max} = V \cdot \Delta^{0.9}$$

where F_{max} = maximum force in MN
V = ship's speed or impact velocity in m/s
Δ = ship's maximum displacement in millions of kilograms

This is the force normal to the hull, and so the vertical bow force component would be the total bow force times the cosine of the angle of the stem bar.

$$F_{vert} = F_{max} \cdot \cos \alpha$$

$$F_{vert} = V \cdot \Delta^{0.9} \cdot \cos \alpha$$

For the POLAR SEA the displacement is close to 11,000 LT (11,170 MT) at the design waterline of 28 ft (8.5 m) and the stem angle 5 feet (1.5 m) below this waterline is about 22.5°. The corresponding values used in the above equation are

$$\Delta = 11.17 \text{ millions of kg}$$
$$\alpha = 22.5°$$

which result in the solid curve on Figure 13. This curve shows Johansson's prediction is a good upper bound for ramming velocities between 3.9 and 8.75 knots (2.0 and 4.5 m/s). It is important to note that Johansson's criteria was intended to include severe ice conditions such as impacting glacial ice, while the ice encountered during the POLAR SEA trials consisted primarily of multiyear ridges and ridge fragments that broke upon impact. These ice conditions probably account for the lower values of bow force.

A second comparison can be made with the full-scale tests conducted onboard the CANMAR KIGORIAK in 1983. The inital test results were reported by Ghoneim, Johansson, Smyth, and Grinstead in Reference 13. They developed an envelope curve for their data which suggests that the bow force is proportional to the square root of the impact velocity.

$$F_{vert} = 2.34 \sqrt{V} \cdot \Delta^{0.9} \cdot \cos \alpha$$

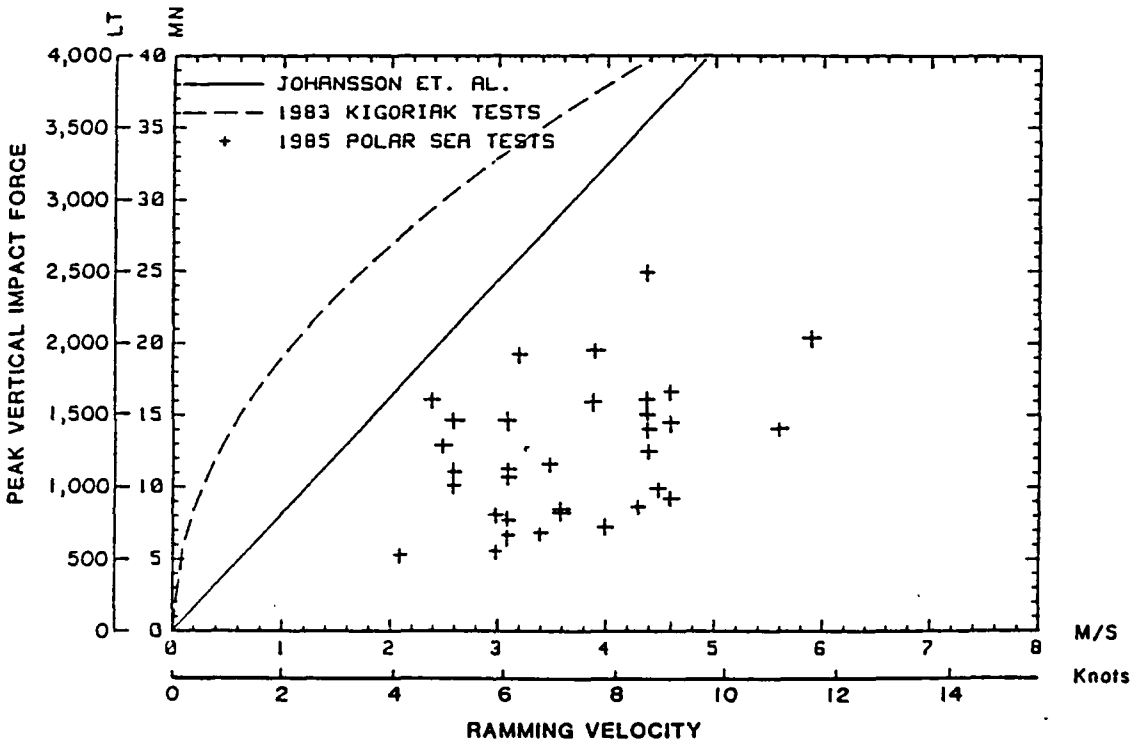

Figure 13

PEAK FORCE vs. VELOCITY RELATIONSHIP

This equation is indicated by the dashed line in Figure 13 with the ship's displacement, Δ, again being given in terms of millions of kg to give a bow force in terms of MN. As a parametric relationship this equation was intended by Ghoneim, et al., to represent only a possible envelope curve based upon the portion of the data they had analyzed. It was not intended to reflect parameters such as bow shape. The ice conditions encountered during the KIGORIAK tests were much more severe than the POLAR SEA experienced with many of the rams being conducted against grounded first year and multiyear ridges. As the graph shows, the KIGORIAK curve certainly does provide an envelope to the POLAR SEA data but it is much higher than Johansson's curve. The lower vertical bow force values obtained during the POLAR SEA tests are again probably due to the lighter ice conditions although it would be difficult to say how much of an effect the different bow shapes may have had.

5.2 Vertical Bow Force Time-Histories

Typical time-history plots of the vertical bow force for the POLAR SEA and the KIGORIAK are illustrated in Figures 14 and 15. Ghoneim and Keinonen [6], in discussing the typical ramming scenario for the KIGORIAK, identify five separate phases. These are the approach phase, the initial impact phase during which the ice crushes and the bow begins to ride up on the ice, the slide up phase, a second impact phase caused by the knife edge contacting the ice, and finally the slide down phase. Figure 15 clearly shows the two impact phases with the bow force dropping from 2360 long tons (23.5 MN) to zero, then rapidly increasing again up to 1200 long tons (12 MN). In this case, the period of zero ice load between the two impacts represents the bow rebounding off the ice surface and results in free vibration of the ship until reloading occurs.

Figure 14 shows a typical time-history plot from the POLAR SEA tests for comparison. After the initial impact of around 1610 long tons (16 MN) the bow force does drop, but it never reaches a state of zero ice load. That is, the bow-ice contact is maintained and the POLAR SEA does not "rebound" as KIGORIAK does. In fact the POLAR SEA bow force time-histories do not show this tendency to rebound on any of the rams analyzed to date. The displacement of the POLAR SEA is almost 1.7 times that of the KIGORIAK which, when coupled with a different bow shape, may explain the difference in the two types of response.

Notice that in the plots for both vessels, a relatively constant force, the beaching force, is achieved at the end of the ram. This is the force that was used earlier in Table 4 for the comparison of hydrostatic beaching force. Also, the impact duration (length of time of the first peak) is approximately 0.48 seconds for the KIGORIAK and 0.8 seconds for the POLAR SEA for these events. Since the rams occurred at different velocities, 4.3 knots (2.3 m/s) for the POLAR SEA and 9.5 knots (4.9 m/s) for the KIGORIAK, a more extensive comparison would have to be done before any conclusion could be reached with regard to a relationship between impact duration and displacement.

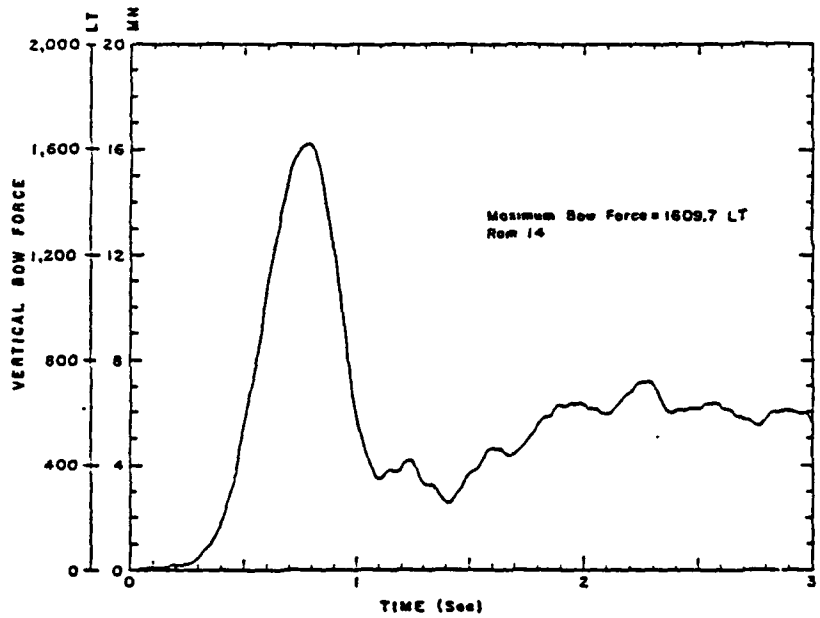

Figure 14

POLAR SEA VERTICAL BOW FORCE TIME HISTORY

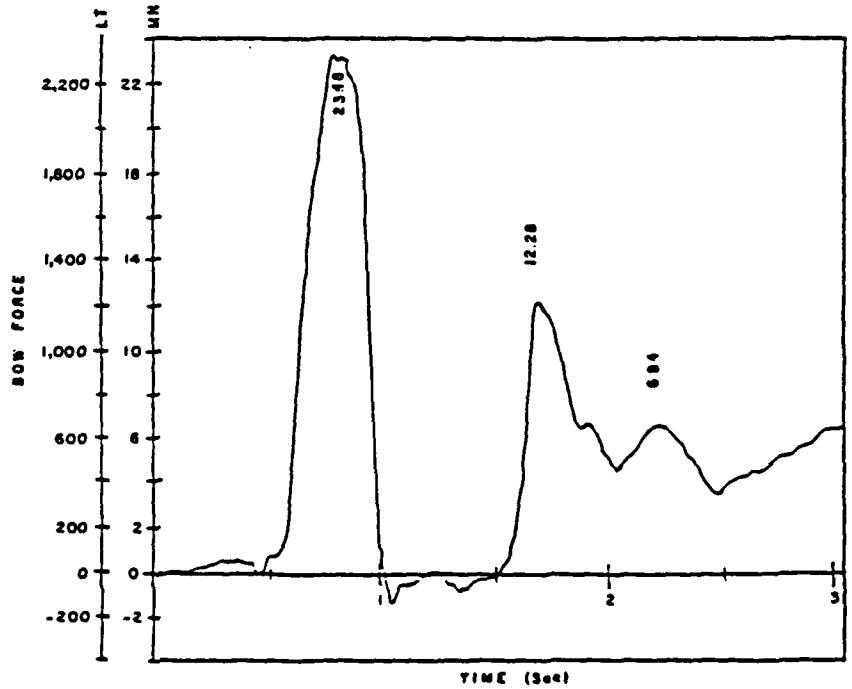

Figure 15

KIGORIAK VERTICAL BOW FORCE TIME HISTORY
(Ram KR426 of Reference 13)

5.3 Longitudinal Bending Moment and Shear Diagrams

The bending moment distributions for the POLAR SEA and the KIGORIAK, at the time of maximum force for a large impact, are shown in Figures 16 and 17 respectively. There are several differences between these graphs. The location of the load on the POLAR SEA is indicated by the vertical arrow which intersects the bending moment curve close to where it crosses the horizontal axis. This location was obtained from the compression gages arrayed along the stem bar and is the location of the gage reading the highest compression. For the KIGORIAK results, a "best match" procedure was employed between the bending moment and shear force diagrams to estimate the center of the load.

The maximum bending moment of the POLAR SEA occurs further forward (approximately 75% of the length of the vessel forward of the stern) than the KIGORIAK's (approximately midships).

The shear distributions for the two ships (for the same rams used in Figures 16 and 17 and at the time of maximum force) are shown in Figures 18 and 19. First note that the sign convention for the shear force is opposite between these two figures. Since bending gages were installed on the POLAR SEA up to cant frame 17, which was forward of the anticipated maximum load location, the bending moment and shear force curves could be calculated forward of the load. In the instrumentation of the KIGORIAK, however, a slightly different approach was used [13]. It was felt that since the bow force was concentrated in the bow area, a frame instrumented to measure the shear force just aft of the load (frame 25 1/2 on the KIGORIAK) would be sufficient. It was assumed that the bending moment forward of the load location had negligible effect on the computations. Once the bending moment and shear curves were obtained up to frame 25 1/2 an extrapolation procedure was used to obtain the bow force at the estimated load location. It is for this reason that Figure 19 does not show any shear up to the bow (frame 30).

Returning to the shear force distribution for the POLAR SEA (Figure 18), it can be seen that around the location of the load the shear changes sign over approximately 50 ft (15 m). This gives a rough indication of the spreading out of the ice load over the extent of the bow. At the point of maximum vertical force, a significant amount of crushing failure has occurred in the ice feature spreading the load over a large contact area.

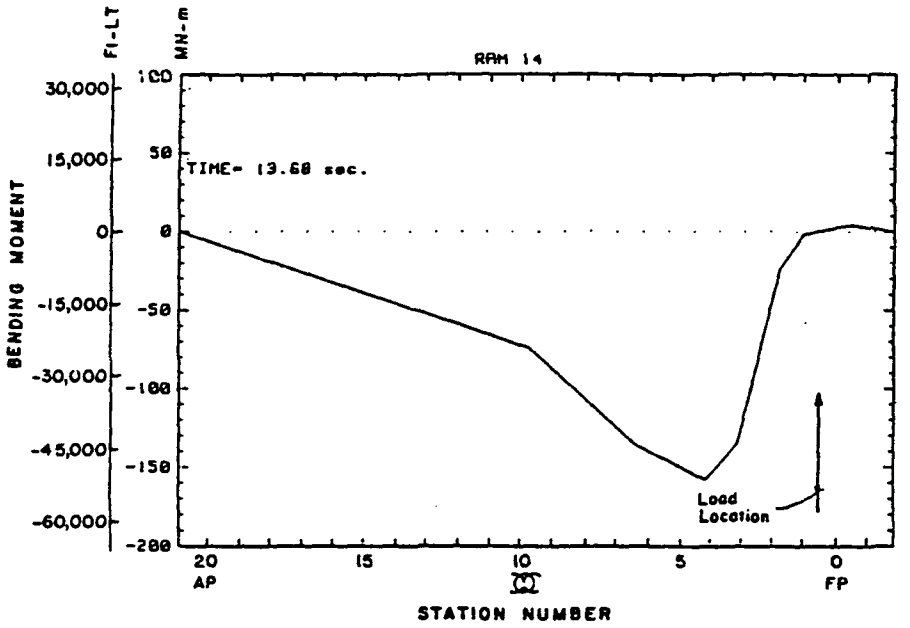

Figure 16
POLAR SEA BENDING MOMENT DISTRIBUTION

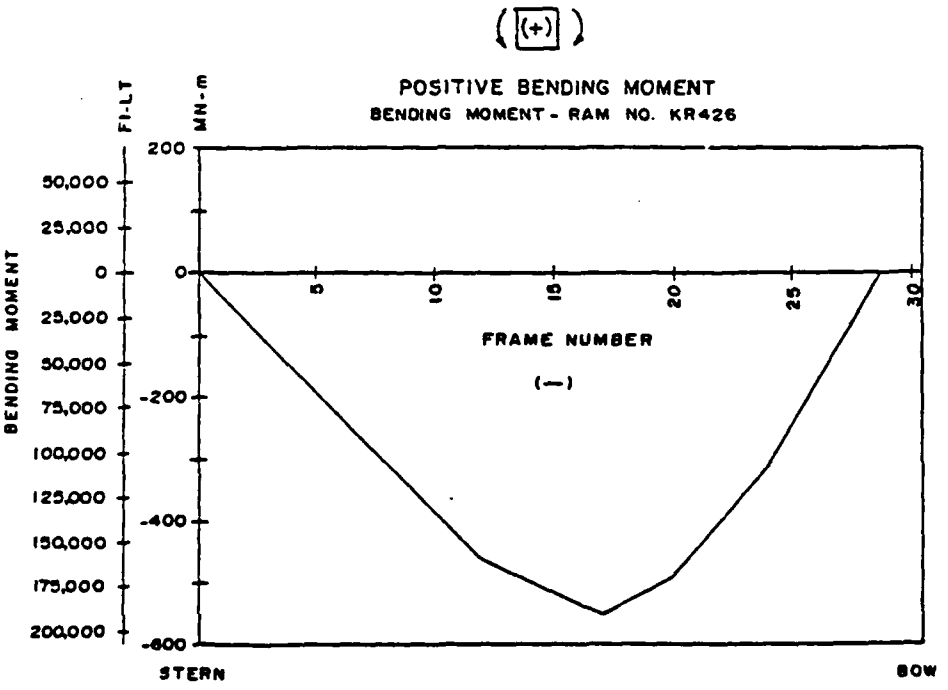

Figure 17
KIGORIAK BENDING MOMENT DISTRIBUTION [13]

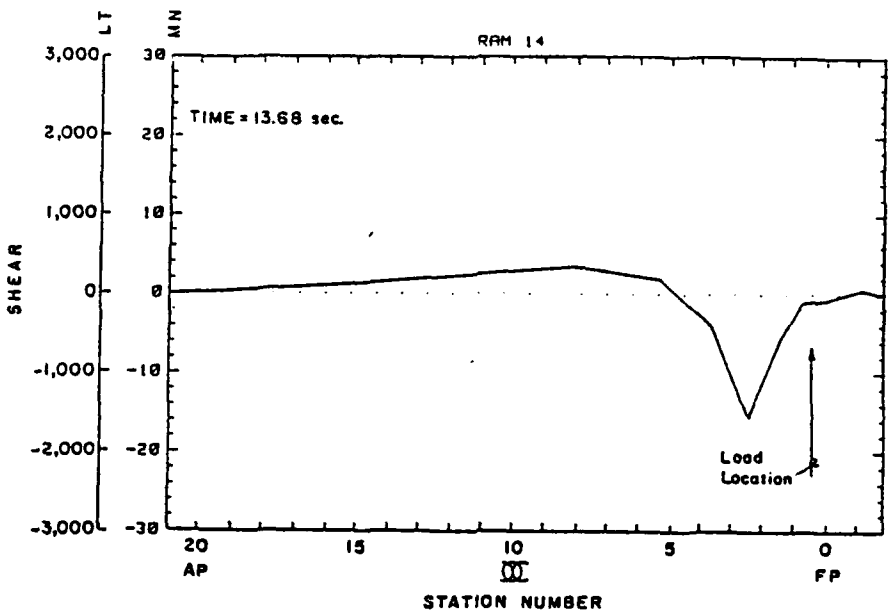

Figure 18
POLAR SEA SHEAR FORCE DISTRIBUTION

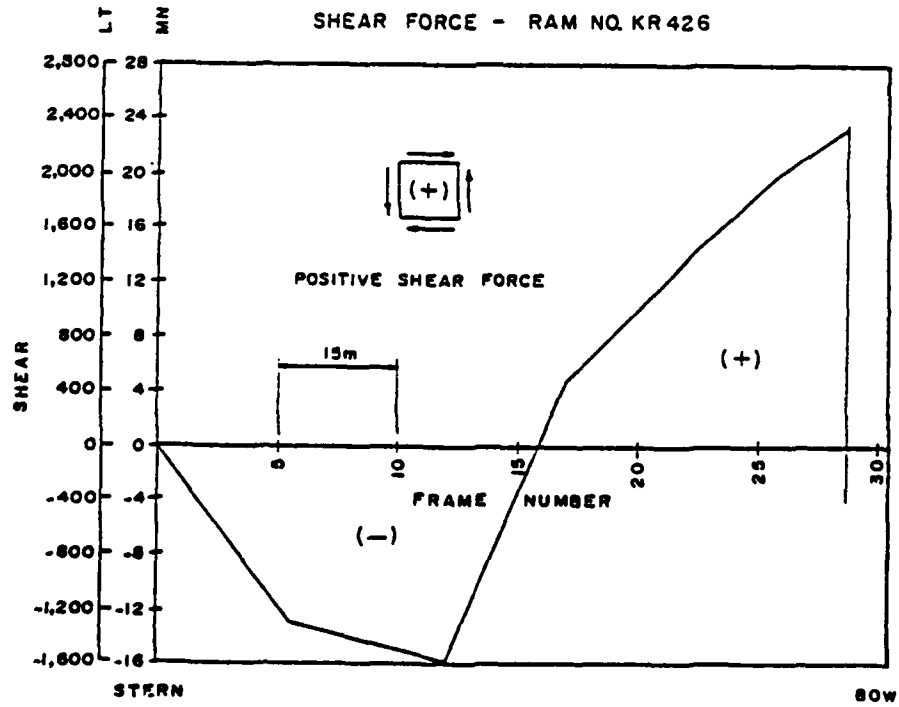

Figure 19
KIGORIAK SHEAR FORCE DISTRIBUTION [13]

6. EVALUATION OF THE ACCURACY OF THE GLOBAL LOAD MEASURING SYSTEM

There are a number of potential sources of error that should be considered in order to estimate the overall accuracy in computing the global bow force. Each of the major errors is investigated in turn and combined with the other errors using the standard techniques of error analysis [19]. Starting with the equation for the bending moment where just the 01 deck bending stress is used and inserting all the variables, we have

$$M = \frac{\sigma \cdot I}{Y} = \frac{\varepsilon \cdot E \cdot I}{Y}$$

$$M = \frac{\varepsilon' \cdot f \cdot E \cdot I}{Y}$$

where f is the transformation factor relating the strain parallel to the deck edge to the principal strain along the centerline and Y is the distance from the neutral axis to the gage elevation at an instrumented frame. The derivation of this equation is contained in Appendix B.

The error associated with measuring the strain, ε', can be estimated from the sampling rate and the accuracy to which peak amplitudes of a signal are measured. Assuming a quarter sine wave with a frequency of 2.5 Hz to represent the rise in strain, as mentioned in Section 2, and using a sampling rate of 100 samples/second, 40 digital samples can be obtained during one cycle at the highest frequency. The digital measurement can therefore occur a maximum of 4.5° away from the peak in the worst case (360°/(40x2)). This yields a maximum error in sampling the peak amplitude of ± 0.31%.

Next, the expression for the transformation factor f contains a $\cos^2\theta$ term where θ is the angle the strain gage is positioned off of the centerline. If the uncertainty in placing the gage and measuring the angle is about 2°, and assuming a θ value of 22° (i.e. near the bow), then the uncertainty in $\cos(\theta)$ is about ± 1.47%. The uncertainty associated with the transformation factor would then be twice this amount.

Uncertainties associated with the moment of inertia, I, are more difficult to determine. For the frames forward of the superstructure inertias were computed manually from the ship's plans and an estimated error of ± 2.5% was used. The neutral axis was judged to be accurate to within ± 0.5 ft. Using a value of 40 feet for the neutral axis near the bow, then the resulting uncertainty is about 1.25%.

Since these uncertainties are based on independent measurements they can be added in quadrature to arrive at the uncertainty in calculating the bending moment.

$$\Delta M/M = [\,(0.31)^2 + (2\text{x}1.47)^2 + (2.5)^2 + (1.25)^2\,]^{0.5}$$

$$= 4.07\%$$

Next, ram number 39, the maximum one recorded, was selected to observe how the uncertainty in the bending moment propagated through the equations for shear and bow force. The 4.07 percent computed above was applied to the four bending moments just fore and aft of the two shear forces used in the calculation of the vertical bow force. The uncertainty for just one of these shear forces is composed of the errors brought about by the uncertainty in the two bending moments. These two errors were added in quadrature.

$$\Delta S_i = [(\Delta M_i / \Delta X)^2 + (\Delta M_{i+1} / \Delta X)^2]^{0.5}$$

Finally, the uncertainty for the two shear forces were also added in quadrature to estimate the uncertainty of the bow force. The final result for ram 39 was as follows:

$$\Delta F = [(\Delta S_i)^2 + (\Delta S_{i+1})^2]^{0.5}$$

$$\Delta F = 246.8 \text{ LT}$$

$$F = 2506 \text{ LT}$$

which implies $\Delta F/F = 9.8\%$

Several other rams were analyzed using the same procedure and in each case the uncertainty was less than 10%. This overall uncertainty, however, takes into account only the errors associated with the measurements of the individual terms that make up the expression for the bending moment. Thus the uncertainty in the measurement of the bending moment applies only to values of the bending moment at the instrumented frames. It does not include any error which may arise from measuring the bending moment at a finite number of points. Therefore an additional uncertainty is present when the shear force distribution is represented by the slope of the straight line segmented bending moment distribution. A more reasonable, but qualitative, assessment of the overall uncertainty in the bow force would probably be ± 15%.

In Section 4 the vertical bow force for two rams was compared to the force obtained from a hydrostatic calculation. The larger error between the two cases was only of the order of 5% which lends credibility to the error estimates computed above.

The error associated with the location of the center of the ice load is unrelated to the uncertainty in estimating the bow force. This was determined from the compression gages installed from cant frames 14 to 38. The spacing of the gages allowed the load center to be estimated with an accuracy of ± 16 in (± 41 cm).

7. CONCLUSIONS

The following is a list of the conclusions from this work:

1. The use of bending gages provided a good estimate of the longitudinal bending moment and shear force distributions. This instrumentation method uses fewer strain gages than attempting to measure the shear force directly.

2. The centerline bulkhead compression gages provided an excellent indication of the location of the center of the ice load. They can also be used to arrive at an estimate for the impact velocity.

3. Global impact ice forces on the POLAR SEA are not localized loads but spread over much of the bow.

4. The superstructure is effective in bending and should not be ignored in design calculations.

5. The maximum bending stress is between the longitudinal location of the forward end of the superstructure and the bottom of the stem.

6. The loading rate was measured to be as high as 5000 LT/s (50 MN/s), considerably less than the KIGORIAK's loading rate of 15000 LT/s (150MN/s) [13].

7. The vessel did not "rebound" after the first impact with the ice as was observed in the KIGORIAK tests [13].

8. The duration of the initial impact phase of a ram is approximately 0.8 seconds for a 4 knot impact velocity.

9. The dominant response of the vessel was at the first mode of vibration (3 Hz).

10. The maximum calculated vertical bow force was 2506 LT (24.97 MN).

11. The maximum bending stress measured was 6078 psi (41.91 MPa) in compression at frame 39 on the 01 deck which is well below the 45,600 psi yield strength for the deck steel.

12. The uncertainty in calculating the bending moment at any of the instrumented frames is approximately ± 4%. The propagation of this error based on a finite number of points results in a bow force uncertainty of ± 10%. Since the bending moment distribution should really be a smooth continuous curve, a reasonable estimate for the overall uncertainty is more likely to be ± 15%.

8. RECOMMENDATIONS

Recommendations based on this study fall into several categories; additional analysis, improvements to the instrumentation, and additional data collection.

Additional analysis can be done with the data already collected to estimate the amount of local ice failure during the ramming event. This report sought the location of the center of the ice load from the stem gage with the maximum compressive strain. These gages could be analyzed in conjunction with the transverse compression gages installed on cant frame 35 to observe how the contact area spreads out during the impact. It is also recommended that further analysis be done on the unsymmetric ramming tests to estimate the transverse force.

Future instrumentation programs aboard the POLAR Class should, wherever possible, shift centerline strain gages outboard to the deck edge. This would reduce the problem of stress concentration influences observed with gages installed near the centerline bulkhead. The data from the two separated gages would be averaged together just as in the case of the 01 deck gages. It would also be desirable to include additional instrumented frames in the bow area of the ship to improve the definition of the shear force distribution over the region of the ice load.

Additional multiyear ice data should be collected with the POLAR Class in order to build up a data base for more complete analysis. In particular, ramming events collected against larger ice features w uld help to validate the possible parameters to be included in any equations describing the maximum bow force versus impact velocity.

REFERENCES

1. "The Canadian Arctic Shipping Pollution Prevention Regulations (CASPPR)", Chapter 33, The Arctic Waters Pollution Prevention Act, Queen's Printer, Ottawa, 1980.

2. P.G. Noble, W.K. Tam, B. Menon and I.M. Bayly, "Ice Forces and Accelerations on a Polar Class Icebreaker", POAC, 1979.

3. G.A.M. Ghoneim and M.W. Smyth, "Finite Element Beam Modelling of Ship Structures under Ice Induced Forces", IAHR Symposium on Ice, Hamburg, August, 1984.

4. Masakatsu Matsuishi, Jun-Ichi Ikeda, Hajime Kawkami, and Masao Hirago, "Ship Ice Floe Collision Analysis Considering the Elastic Deflection of Hull Girder", Ice-Tech 84, SNAME, Calgary, May, 1984.

5. P. Varsta, "Modelling of Impact between Ship Hull and Ice", POAC 83, Vol. 2, pp. 760-777.

6. G.A.M. Ghoneim and A.J. Keinonen, "Full Scale Impact Tests of Canmar Kigoriak In Thick Ice", POAC, April 1983.

7. G.A.M. Ghoneim, M.H. Edgecombe, and J. Grinstead, "System Development for Measurement of Full Scale Ship Ice Impact Forces", Ice-Tech 84, SNAME, May 1984.

8. A.J. Keinonen, "Ice Loads on Ships in the Canadian Arctic", WEGEMT, 1983.

9. A. Churcher, A. Kolomocjev, and G. Hubbard, "Design of the Robert LeMeur Ice Breaking Supply Ship", SNAME, Pacific Northwest Section, Vancouver, 1983.

10. S.H. Iyer, "Calibration Testing of M.V. Arctic for the Measurement of Icebreaking Loads", Workshop on Sea Ice Field Measurement, St. John's, Newfoundland, April 29 -May 01, 1980.

11. I.F. Glen, and C. Daley, "Ice Impact Loads on Ships", Arctic Section, SNAME, Calgary, May 1982.

12. I.F. Glen, C. Daley, J. Edworthy, and G. Gareau, "Studies Supporting Update of the CASPPR Regulations Group 1 and 2", Report 586A by Arctec Canada Limited for Canadian Coast Guard, 1982.

13. G.A.M. Ghoneim, B.M. Johansson, M.W. Symth, J. Grinstead, "Global Ship Ice Impact Forces Determined from Full-Scale Tests and Analytical Modelling of the Icebreakers Canmar Kigoriak and Robert LeMeur," TSNAME, November 1984.

14. B.M. Johansson, A.J. Keinonen, and B. Mercer, "Technical Development of an Environmentally Safe Arctic Tanker", Ice Tech 81, SNAME Spring Meeting/Star Symposium, Ottawa, June 1981.

15. J.W. St. John, C. Daley and H. Blount, "Ice Loads and Ship Response to Ice", Report SR-1291 by ARCTEC, Incorporated and ARCTEC CANADA Limited for U.S. Maritime Administration, Ship Structure Committee, and The Canadian Transport Development Center, 1984.

16. I.F. Glen, I. Majid, G. Tam, and B. Menon, "Winter 1981 Trafficability Tests of the Polar Sea," Volume IX "Ice Induced Vibration Measurements and Development of a Model for Icebreaking Excitation Forces," ARCTEC CANADA Limited Report No. 792C-5, ARCTEC, Incorporated, Report No. 583C-3, April, 1982.

17. H. Blount, I.F. Glen, G. Comfort, and G. Tam, "Results of Full Scale Measurements aboard CCGS Louis S. St. Laurent During a 1980 Fall Arctic Probe," Volume 1, ARCTEC CANADA Limited, Report No. 737C for Canadian Ccoast Guard, July 1981.

18. M.G. Harrington, and J.W. St. John, "Environmental Data Collection aboard USCGC Polar Sea, 1985," Volume I "Environmental Data," ARCTEC ENGINEERING, Inc., Report No. 1095C, November 1986.

19. H. Schenck, Jr., "Theories of Engineering Experimentation," McGraw-Hill Book Company, Inc., New York, 1961.

APPENDIX A

SENSOR/CHANNEL SPECIFICATIONS AND LOCATIONS

This appendix gives some of the specific details associated with the operation and installation of the data acquisition system onboard the POLAR SEA.

In the initial configuration of the system maximum expected values had to be estimated for the strains and other engineering quantities in order to calibrate and interpret the measurements received. Using the strain gages as an example, it was estimated that the maximum peak strain expected to occur with the highest impact loads was approximately 500 microstrain. This full scale value was used to adjust the the gain setting on the signal filter/amplifiers to provide a maximum output of $\pm$10 volts to a analog-to-digital subsystem. The A-to-D system used was a HP 6940B Multiprogrammer with enough scanning boards to handle up to 48 channels of data. Associated with the analog-to-digital process was a conversion factor of 10 volts/2000 A-to-D units which places some limits on the resolution of the resulting data. For a full scale of 497.512 microstrain/10 volts on all the strain gages this resolution corresponds to a value of 0.2487 microstrain/A-to-D unit. A similar procedure was carried out for the accelerometers and the doppler velocity radar to arrive at the calibration factors listed in Tables A1 and A2. All of the strain gages were wired as opposite-active arm bridges and had an excitation of 10 volts.

The control, storage and processing data collection functions were performed by the Hewlett-Packard series 200 model 9816 desk top computer with an internal memory of approximately 4.3 megabytes. The computer was used to program and receive the data from the HP 6940B Multiprogrammer. Prior to each ramming event the computer programmed the HP 6940B so that it would scan through all of its 48 data channels (including some null channels) 100 times each second for 25 seconds. When the proper cue was received from the computer the scanning would commence. With each scan the multiprogrammer received the filtered data, converted it to digital form, and transfered it to the computer's memory. Afterwards the measurements were transfered from computer memory onto a 3.5 inch floppy disk for storage; one ram event for each disk.

The signal processing filters, analog-to-digital multiprogrammer, and the computer were all set up in the windlass room aboard the POLAR SEA. This compartment was selected because of its central location with respect to laying of the necessary cables to each of the strain gages, and because the out of the way location would not interfere with shipboard activities. The equipment rack also contained a video screen giving the view from aloft conn of the bow of the vessel and the area forward of the bow. Extra components were available for the entire system in case the failure of one or more of the essential elements occurred.

The installation of electronic equipment and strain gages onboard the POLAR SEA was carried out in July of 1985; approximately two months prior to the deployment. After arrival in the Beaufort Sea and before any ramming tests were conducted the entire system was checked out. This investigation led to four strain gages that were found to be defective (probably due to water exposure). Three of the gages were located on the 01 weather deck and replaced. The fourth was one of the centerline compression gages used to locate the ice load along the stem bar. Unfortunately, it was located in the lowest part of the 3-E-O-W tank and frozen beneath two feet of ice. It was judged that ample load locating capability was provided by the rest of the compression gages and so no attempt was made to replace it. The refurbished gage system was found to provide clean, noise free data with a worst case noise of less than 20 millivolts in a $\pm$10 volt range.

TABLE A1

POLAR SEA IMPACT TESTS FALL 1985

SENSOR SPECIFICATIONS FOR RAMS 1 AND 2

CHAN #	CHAN ID	CALIBRATION FACTOR	GAGE FACTOR	EXIT. VOLTAGE	BRIDGE TYPE	UNITS
1	C-C24	2.487E-6	2.01	10.00	2.00	strain
2	C-C26	2.487E-6	2.01	10.00	2.00	strain
3	C-C28	2.487E-6	2.01	10.00	2.00	strain
4	C-C30	2.487E-6	2.01	10.00	2.00	strain
5	C-C32	2.487E-6	2.01	10.00	2.00	strain
6	C-C34	2.487E-6	2.01	10.00	2.00	strain
7	C-C36	2.487E-6	2.01	10.00	2.00	strain
8	C-C38	2.487E-6	2.01	10.00	2.00	strain
9	S-C27	2.487E-6	2.01	10.00	2.00	strain
10	S-C35	2.487E-6	2.01	10.00	2.00	strain
11	B3-C35C	2.487E-6	2.01	10.00	2.00	strain
12	B3-C44C	2.487E-6	2.01	10.00	2.00	strain
13	B2-C17C	2.487E-6	2.01	10.00	2.00	strain
14	C-C20	2.487E-6	2.01	10.00	2.00	strain
15	C-C18	2.487E-6	2.01	10.00	2.00	strain
16	C-C16	2.487E-6	2.01	10.00	2.00	strain
17	C-C14	2.487E-6	2.01	10.00	2.00	strain
18	B01-C17-P	2.487E-6	2.01	10.00	2.00	strain
19	B01-C27-P	2.487E-6	2.01	10.00	2.00	strain
20	B01-C35-P	2.487E-6	2.01	10.00	2.00	strain
21	B01-C44-P	2.487E-6	2.01	10.00	2.00	strain
22	B01-39-P	2.487E-6	2.01	10.00	2.00	strain
23	B01-55-P	2.487E-6	2.01	10.00	2.00	strain
24	B01-86-P	2.487E-6	2.01	10.00	2.00	strain
25	B01-128-P	2.487E-6	2.01	10.00	2.00	strain
26	B3-39C	2.487E-6	2.01	10.00	2.00	strain
27	M-V (speed)	1.097E-2	0.00	6.09	0.00	knots
28	M-A-T (sway)	6.225E-4	0.00	28.00	0.00	g
29	M-A-L (surge)	6.185E-4	0.00	28.00	0.00	g
30	M-A-V (heave)	1.236E03	0.00	28.00	0.00	g
31	C-C35-9P	2.487E-7	2.01	10.00	2.00	strain
32	C-C35-10S	2.487E-7	2.01	10.00	2.00	strain
33	C-C35-10P	2.487E-7	2.01	10.00	2.00	strain
34	C-C34-11S	2.487E-7	2.01	10.00	2.00	strain
35	C-C35-11P	2.487E-7	2.01	10.00	2.00	strain
36	B1P-C44C	2.487E-7	2.01	10.00	2.00	strain
37	B01-C17-S	2.487E-7	2.01	10.00	2.00	strain
38	B01-C27-S	2.487E-7	2.01	10.00	2.00	strain
39	B01-C35-S	2.487E-7	2.01	10.00	2.00	strain
40	B01-C44-S	2.487E-7	2.01	10.00	2.00	strain
41	B01-39-S	2.487E-7	2.01	10.00	2.00	strain
42	B01-55-S	2.487E-7	2.01	10.00	2.00	strain
43	B01-86-S	2.487E-7	2.01	10.00	2.00	strain
44	B01-128-S	2.487E-7	2.01	10.00	2.00	strain
45	B3-55-P	2.487E-7	2.01	10.00	2.00	strain
46	B3-55-S	2.487E-7	2.01	10.00	2.00	strain
47	NULL					
48	NULL					

TABLE A2

POLAR SEA IMPACT TESTS FALL 1985

SENSOR SPECIFICATIONS FOR RAMS 3 TO 40

CHAN #	CHAN ID	CALIBRATION FACTOR	GAGE FACTOR	EXIT. VOLTAGE	BRIDGE TYPE	UNITS
1	C-C24	2.487E-7	2.01	10.00	2.00	strain
2	C-C26	2.487E-7	2.01	10.00	2.00	strain
3	C-C28	2.487E-7	2.01	10.00	2.00	strain
4	C-C30	2.487E-7	2.01	10.00	2.00	strain
5	C-C32	2.487E-7	2.01	10.00	2.00	strain
6	C-C34	2.487E-7	2.01	10.00	2.00	strain
7	C-C36	2.487E-7	2.01	10.00	2.00	strain
8	C-C38	2.487E-7	2.01	10.00	2.00	strain
9	S-C27	2.487E-7	2.01	10.00	2.00	strain
10	S-C35	2.487E-7	2.01	10.00	2.00	strain
11	B3-C35C	2.487E-7	2.01	10.00	2.00	strain
12	B3-C44C	2.487E-7	2.01	10.00	2.00	strain
13	B2-C17C	2.487E-7	2.01	10.00	2.00	strain
14	C-C20	2.487E-7	2.01	10.00	2.00	strain
15	C-C18	2.487E-7	2.01	10.00	2.00	strain
16	C-C16	2.487E-7	2.01	10.00	2.00	strain
17	C-C14	2.487E-7	2.01	10.00	2.00	strain
18	BO1-C17-P	2.487E-7	2.01	10.00	2.00	strain
19	BO1-C27-P	2.487E-7	2.01	10.00	2.00	strain
20	BO1-C35-P	2.487E-7	2.01	10.00	2.00	strain
21	BO1-C44-P	2.487E-7	2.01	10.00	2.00	strain
22	BO1-39-P	2.487E-7	2.01	10.00	2.00	strain
23	BO1-55-P	2.487E-7	2.01	10.00	2.00	strain
24	BO1-86-P	2.487E-7	2.01	10.00	2.00	strain
25	BO1-128-P	2.487E-7	2.01	10.00	2.00	strain
26	B3-39C	2.487E-7	2.01	10.00	2.00	strain
27	M-V	1.097E-2	0.00	6.09	0.00	knots
28	M-A-T	6.225E-4	0.00	28.00	0.00	g
29	M-A-L	6.185E-4	0.00	28.00	0.00	g
30	M-A-V	1.236E03	0.00	28.00	0.00	g
31	C-C35-9P	2.487E-7	2.01	10.00	2.00	strain
32	C-C35-10S	2.487E-7	2.01	10.00	2.00	strain
33	C-C35-10P	2.487E-7	2.01	10.00	2.00	strain
34	C-C34-11S	2.487E-7	2.01	10.00	2.00	strain
35	C-C35-11P	2.487E-7	2.01	10.00	2.00	strain
36	B1P-C44C	2.487E-7	2.01	10.00	2.00	strain
37	BO1-C17-S	2.487E-7	2.01	10.00	2.00	strain
38	BO1-C27-S	2.487E-7	2.01	10.00	2.00	strain
39	BO1-C35-S	2.487E-7	2.01	10.00	2.00	strain
40	BO1-C44-S	2.487E-7	2.01	10.00	2.00	strain
41	BO1-39-S	2.487E-7	2.01	10.00	2.00	strain
42	BO1-55-S	2.487E-7	2.01	10.00	2.00	strain
43	BO1-86-S	2.487E-7	2.01	10.00	2.00	strain
44	BO1-128-S	2.487E-7	2.01	10.00	2.00	strain
45	B3-55-P	2.487E-7	2.01	10.00	2.00	strain
46	B3-55-S	2.487E-7	2.01	10.00	2.00	strain
47	NULL					
48	NULL					

TABLE A3

POLAR SEA IMPACT TESTS FALL 1985

SENSOR LOCATIONS

CHAN#	CHAN ID	LONG ft	LONG (m)	VERT ft	VERT (m)
1	C-C24	372.0	113.4	29.9	9.1
2	C-C26	362.5	110.5	29.2	8.9
3	C-C28	359.3	109.5	27.9	8.5
4	C-C30	356.3	108.6	26.9	8.2
5	C-C32	353.3	107.7	25.9	7.9
6	C-C34	350.3	106.8	24.6	7.5
7	C-C36	348.1	106.1	23.6	7.2
8	C-C38	344.5	105.0	22.0	6.7
9	S-C27	360.9	110.0	26.9	8.2
10	S-C35	348.8	106.3	22.6	6.9
11	B3-C35C	348.8	106.3	29.2	8.9
12	B3-C44C	335.6	102.3	29.2	8.9
13	B2-C17C	376.0	114.6	37.4	11.4
14	C-C20	371.4	113.2	30.8	9.4
15	C-C18	374.3	114.1	32.2	9.8
16	C-C16	377.3	115.0	32.2	9.8
17	C-C14	380.2	115.9	33.5	10.2
18	B01-C17-P	376.0	114.6	59.4	18.1
19	B01-C27-P	360.9	110.0	58.7	17.9
20	B01-C35-P	348.8	106.3	58.4	17.8
21	B01-C44-P	335.6	102.3	57.7	17.6
22	B01-39-P	316.9	96.6	56.8	17.3
23	B01-55-P	294.6	89.8	56.1	17.1
24	B01-86-P	253.6	77.3	54.8	16.7
25	B01-128-P	196.9	60.0	53.1	16.2
26	B3-39C	316.9	96.6	28.5	8.7
27	M-V	193.6	59.0	52.5	16.0
28	M-A-T	369.1	112.5	49.5	15.1
29	M-A-L	369.1	112.5	49.5	15.1
30	M-A-V	369.1	112.5	49.5	15.1
31	C-C35-9P	348.8	106.3	25.9	7.9
32	C-C35-10S	348.8	106.3	24.6	7.5
33	C-C35-10P	348.8	106.3	24.6	7.5
34	C-C34-11S	348.8	106.3	23.3	7.1
35	C-C35-11P	348.8	106.3	23.3	7.1
36	B1P-C44C	335.6	102.3	21.0	6.4
37	B01-C17-S	376.0	114.5	59.4	18.1
38	B01-C27-S	360.9	110.0	58.7	17.9
39	B01-C35-S	348.8	106.3	58.4	17.8
40	B01-C44-S	335.6	102.3	57.7	17.6
41	B01-39-S	316.9	96.6	56.8	17.3
42	B01-55-S	294.6	89.8	56.1	17.1
43	B01-86-S	254.9	77.7	54.8	16.7
44	B01-128-S	196.9	60.0	53.1	16.2
45	B3-55-P	294.6	89.8	27.9	8.5
46	B3-55-S	294.6	89.8	27.9	8.5

APPENDIX B

DETAILS OF THE ANALYSIS PROCEDURE

CALCULATION OF BENDING STRESS

$$\sigma(\text{Rdg}) = [(\text{Data}(\text{Rdg}, \text{Chn}) - \text{Base-line}\ (\text{Chn})] \times (\text{Calib}(\text{Chn})) \times (f) \times (E)$$

σ(Rdg)	=	Bending Stress Rdg= Reading number (100/second)
Data (Rdg, Chn)	=	Data from A/D Subsystem Chn = Channel number (42 channels)
Base-line (Chn)	=	Base line, calculated as the average of 100 readings before impact occurs.
Calib (Chn)	=	Calibration constant (converts A/D counts to strain).
E	=	Elastic Modulus 30 x 10^6 psi (2.07E+11 Pa)
f	=	Factor for transformation of stress parallel to side shell to stress parallel to center line of vessel.

The transformation factor f which relates the stress parallel to the deck edge to the principal stress parallel to the centerline was calculated from the equation for strain at a point.

$$\varepsilon x' = \varepsilon x \cdot (\cos\theta)^2 + \varepsilon y \cdot (\sin\theta)^2 + \gamma \cdot \sin\theta \cdot \cos\theta$$

If εx and εy are the strains in the principal directions, then the shearing strain, γ, is equal to zero. In this case it is assumed that the principal strain εx lies along or is very close to the centerline of the ship.

$$\varepsilon x' = \varepsilon x \cdot (\cos\theta)^2 + \varepsilon y \cdot (\sin\theta)^2$$

$$\varepsilon x' = \varepsilon x \cdot (\cos\theta)^2 + \varepsilon y \cdot (1 - (\cos\theta)^2)$$

Using $\varepsilon y = - \upsilon \cdot \varepsilon x$

$$\varepsilon x' = \varepsilon x \cdot (\cos\theta)^2 - \upsilon \cdot \varepsilon x \cdot (1 - (\cos\theta)^2)$$

$$\varepsilon x' = \varepsilon x \cdot [(\cos\theta)^2 \cdot (1 + \upsilon) - \upsilon]$$

$$\varepsilon x = \varepsilon x' / [(\cos\theta)^2 \cdot (1 + \upsilon) - \upsilon]$$

$$\varepsilon x = \varepsilon x' \cdot f$$

where $\varepsilon x'$ = measured strain parallel to side shell
εx = principal strain parallel to the centerline
γ = shear strain = 0
θ = angle between the ship's centerline and the tangent line to side shell at the gage location
υ = Poisson's ratio = 0.29

Next Hooke's law for a plane stress state is used with the assumption that for the ship in bending the stress in the transverse direction is much less than the longitudinal stress. Therefore

$$\sigma(Rdg) = \varepsilon x \cdot E$$

$$\sigma(Rdg) = \varepsilon x' \cdot f \cdot E$$

CALCULATION OF BENDING MOMENT

Frame 55 $M=(\varepsilon 2-\varepsilon 3)x(E)x(I)/D$

Frames 39,86,128
Cant frames 17,27,35,44 $M=(\varepsilon 01)x(E)x(I)/Y$

M = bending moment (negative if 01 deck is in compression)

$\varepsilon 01$ = average bending strain in 01 deck at instrumented frame

$\varepsilon 2$ = average bending strain in 2nd deck at instrumented frame

$\varepsilon 3$ = average bending strain in 3rd deck at instrumented frame

E = elastic modulus of the deck plating

I = transverse sectional inertia

Y = distance from the neutral axis to the 01 deck

D = vertical distance between gages located at the same frame

NOTE: The deck bending gages located on the centerline were not used in the bending moment calculation, because local stress fields occurred when the ice force was located at the frame containing these gages.

CALCULATION OF SHEAR FORCE VALUES

$$S(X) = -(M2-M1)/(X2-X1)$$

S(x)	=	the shear force at x=X1 + (X2-X1)/2
M1	=	the bending moment at x=X1
M2	=	the bending moment at x=X2
X1	=	the longitudinal location of bending moment M1
X2	=	the longitudinal location of bending moment M2

LOCATION OF THE CENTER OF THE LOAD

$$Loc = Loc\_comp(Max\_comp)$$

The location of the center of the ice load was taken to be at the location of the stem bar compression gage undergoing the largest amount of compression.

CALCULATION OF VERTICAL FORCE ON THE BOW

A. If bending gages forward of location of load

Bow_f	=	ABS [S(x1)] + ABS [S(x2)]
Bow_f	=	the vertical ice force on the bow
S(x1)	=	shear force aft of the location of the load
S(x2)	=	shear force forward of the location of the load
ABS	=	absolute value of quantity in brackets

B. If no bending gages forward of location of load

Bow_f = ABS[S(x1)]+(Mass)x(acc) ≈ ABS(S(x1))

Bow_f = vertical ice force on bow

S(x1) = shear aft of location of load

Mass = mass of bow section forward of ice force

acc = vertical acceleration of bow section

NOTE: The maximum inertial force [(mass)x(ACC)], for the case of no bending gages forward of the location of the load, is approximately 30 LT (0.3 MN).

CALCULATION OF BEACHING FORCE FROM HYDROSTATICS

Beach f = $\sin\phi$ · LBP · MTI/d

= beaching force on the bow in long tons

ϕ = trim angle

LBP = length between perpendiculars (inches)

MTI = moment to trim one inch

= 925 ft-LT (at a draft of 28 ft)

d = distance from the ice force to the longitudinal center of floation

≈ 158 ft

The vessel's angle of trim when all headway was stopped during a ramming event was estimated from the accelerometer measuring the longitudinal acceleration. Before the ram the heave accelerometer indicates a 1g acceleration while the sway and surge accelerometers indicate zero acceleration. With the vessel in the beached condition, however, the heave and surge accelerometers give two components to the downward 1g gravitational acceleration.

$$\sin\phi \approx ax(\text{measured in g's})/1g = ax$$

APPENDIX C

DESCRIPTION OF THE GLOBAL LOAD ANALYSIS SOFTWARE

General Description

The program developed for the USCGC POLAR SEA Impact Tests was derived from the program written for the M.V. KIGORIAK and the M.V. ROBERT LEMEUR Impact Tests conducted in 1983. The main function of the program is to calculate and plot the global vertical load time history on the bow of the POLAR SEA. The following calculations can be performed by the program:

- longitudinal shear force and bending moment distribution
- neutral axis location
- vertical ice force on bow
- cubic spline curve fitting
- maximum and minimum values calculated
- longitudinal location of maximum and minimum bending and shear values
- location of center of ice load on bow

The analysis software was quite versatile in its mode of application. While a full length report containing everything from graphs of the output from each strain gage to the final time-history of the vertical bow force took about a hour to generate, the program allowed for much quicker results if desired. Once the data disk was read by the computer, any of the strain gage time histories could be viewed and plotted. Also, any time segment out of the 25 second sampling interval could be selected for calculation of the bending moment, shear, or bow force to be displayed and/or plotted. This latter mode of operation reduced the computations down to a few minutes and was used primarily during the system checkout phase to determine operational readiness of the instrumentation.

The hardware required for the analysis program is as follows:

- HP 9816 Computer
- HP 9121 Disk Drive
- HP 2225A Think Jet Printer
- 2.2 MBytes of Memory

The HP Basic 3.0 operating system is required also.

A general soft key menu flow chart is illustrated in Figure C1.

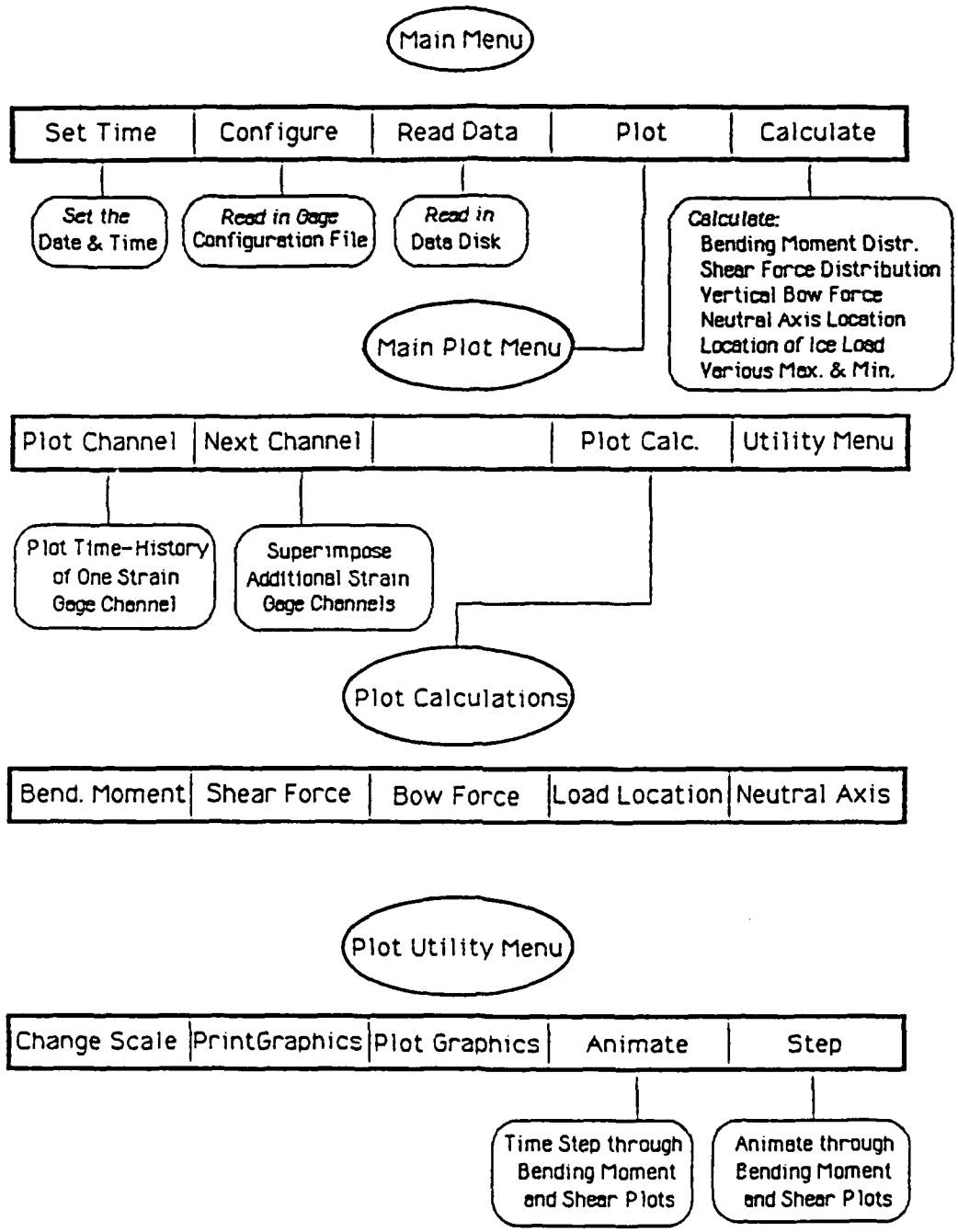

Figure C1

GLOBAL LOAD ANALYSIS FLOWCHART

APPENDIX D

REPRESENTATIVE SAMPLES OF DATA

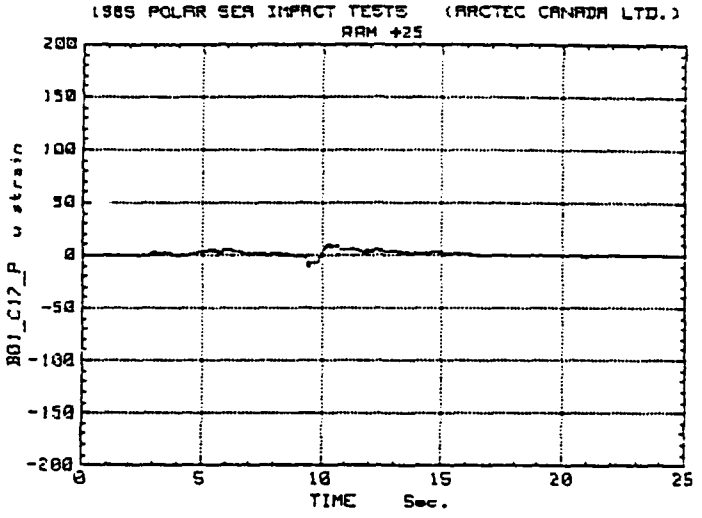

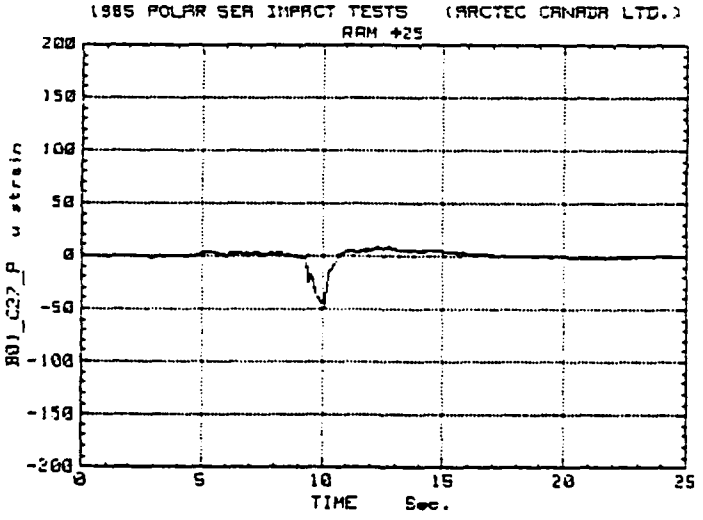

PROGRAM USED: CALC1
ANALYSIS DATE/TIME: 20 Jan 1986/16:41:39
ACQUISTION DATE/TIME: 10 Oct 1985/18:01:55

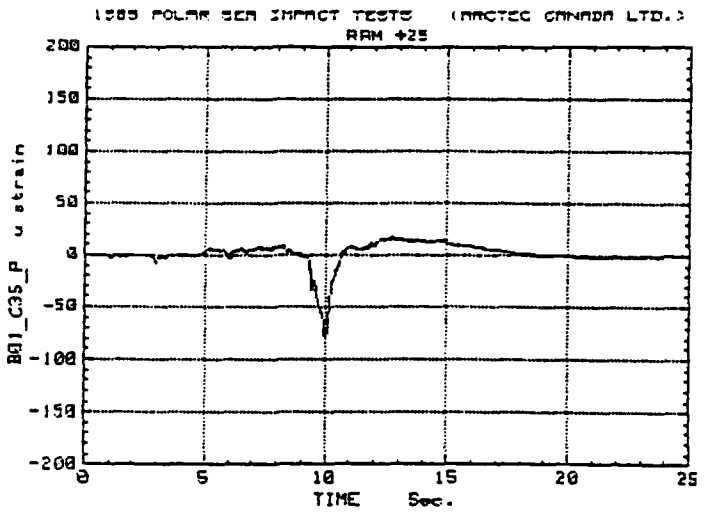

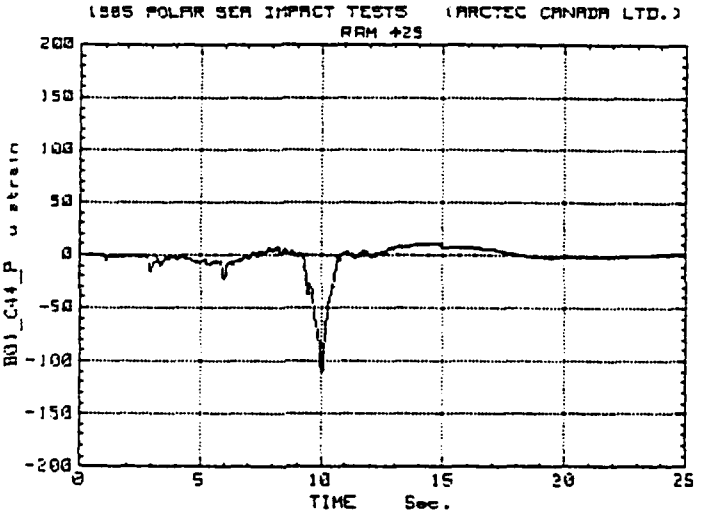

PROGRAM USED: CALC1
ANALYSIS DATE/TIME: 20 Jan 1986/16:42:52
ACQUISTION DATE/TIME: 10 Oct 1985/18:01:55

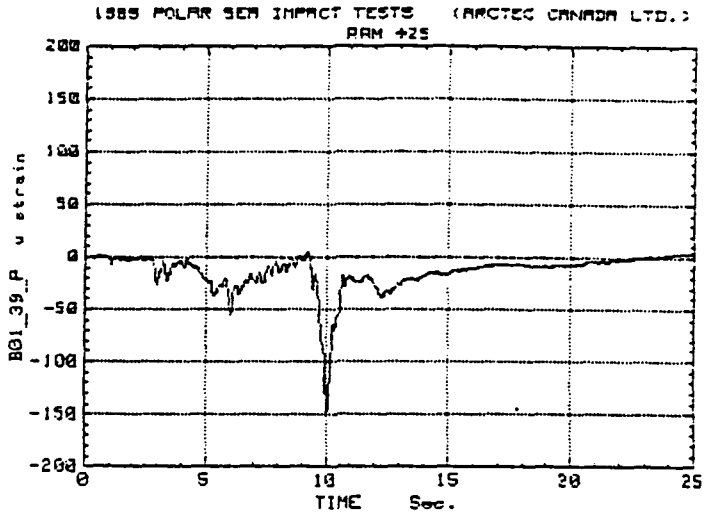

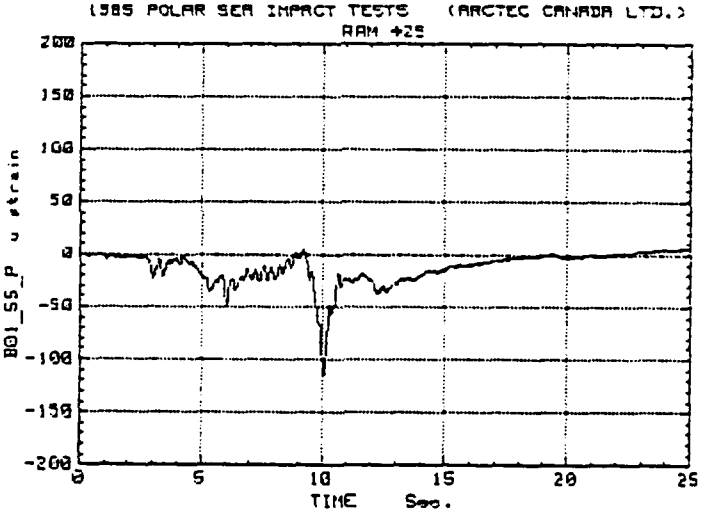

PROGRAM USED: CALC1
ANALYSIS DATE/TIME: 20 Jan 1986/16:44:05
ACQUISTION DATE/TIME: 10 Oct 1985/18:01:55

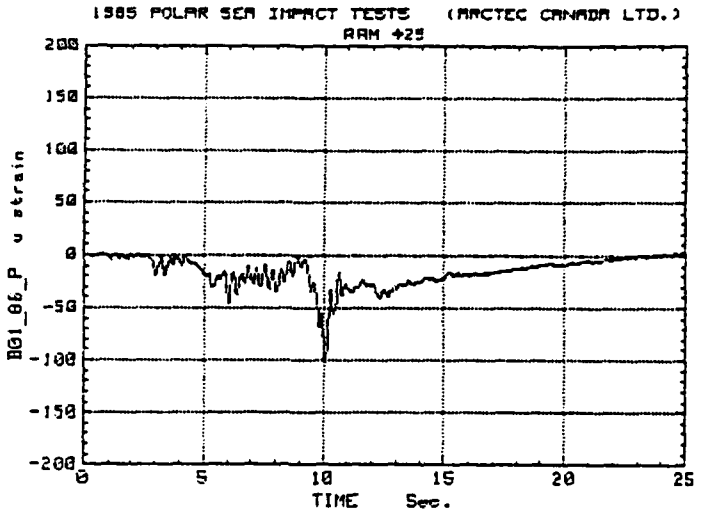

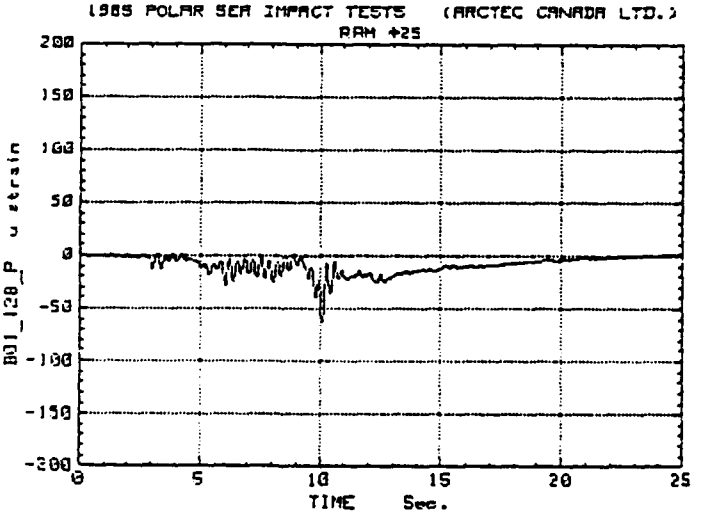

PROGRAM USED: CALC1
ANALYSIS DATE/TIME: 20 Jan 1986/16:45:18
ACQUISTION DATE/TIME: 10 Oct 1985/18:01:55

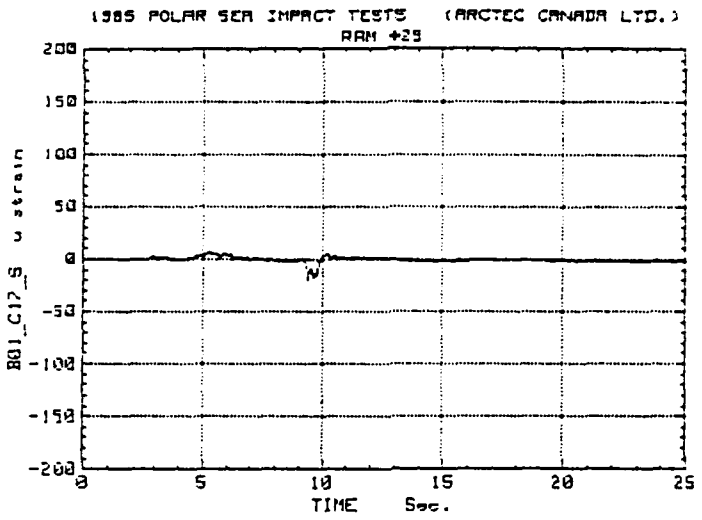

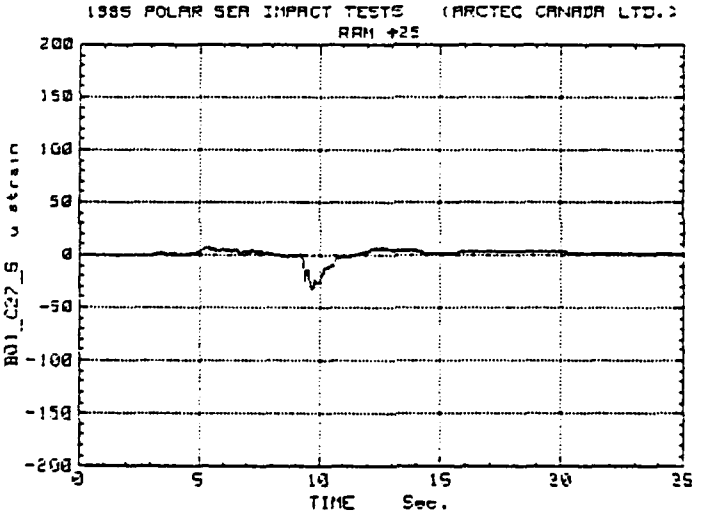

PROGRAM USED: CALC1
ANALYSIS DATE/TIME: 20 Jan 1986/16:46:31
ACQUISTION DATE/TIME: 10 Oct 1985/18:01:55

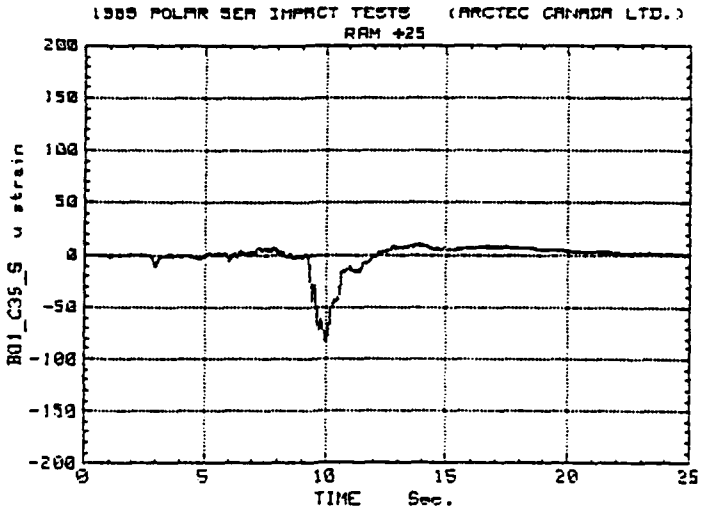

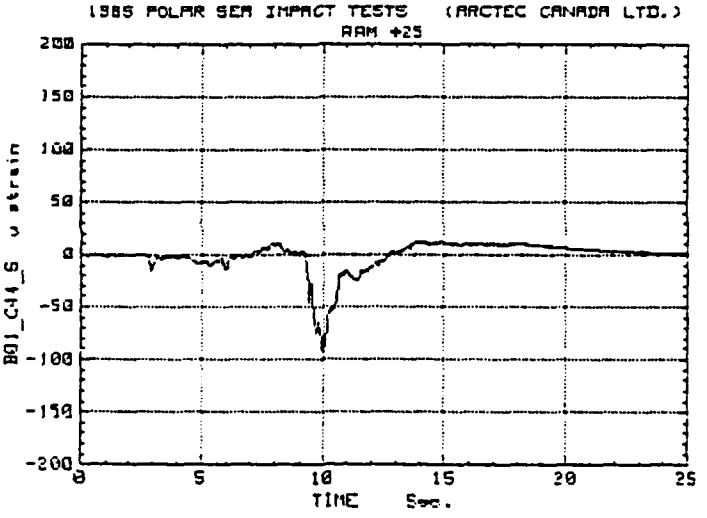

PROGRAM USED: CALC1
ANALYSIS DATE/TIME: 20 Jan 1986/16:47:44
ACQUISTION DATE/TIME: 10 Oct 1985/18:01:55

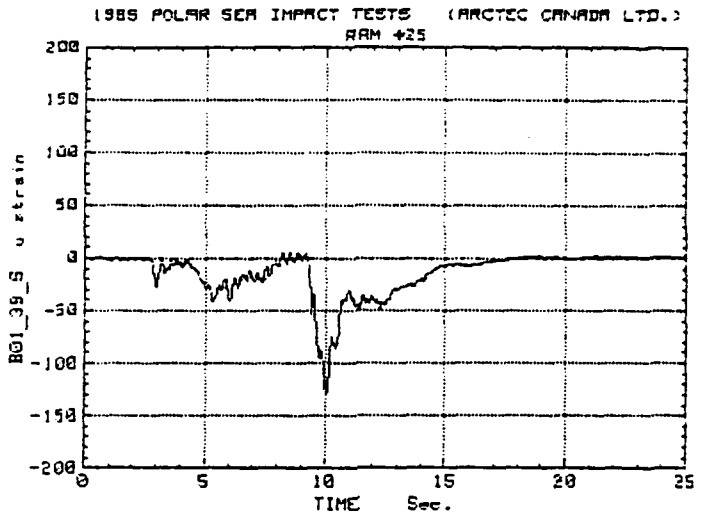

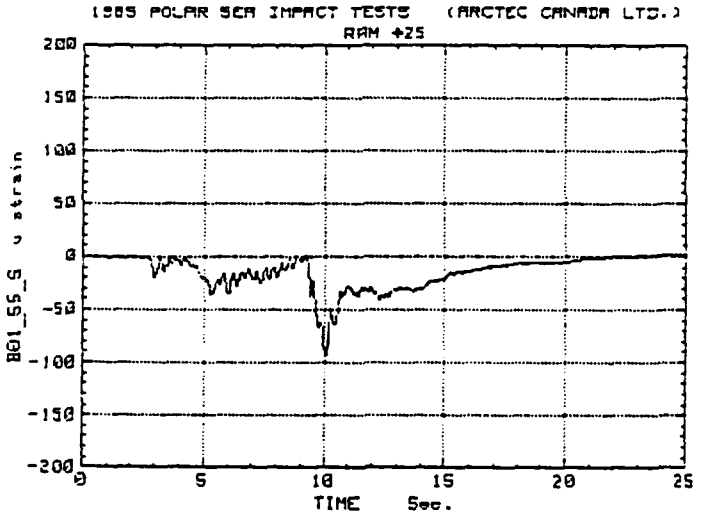

PROGRAM USED: CALC1
ANALYSIS DATE/TIME: 20 Jan 1986/16:48:57
ACQUISTION DATE/TIME: 10 Oct 1985/18:01:55

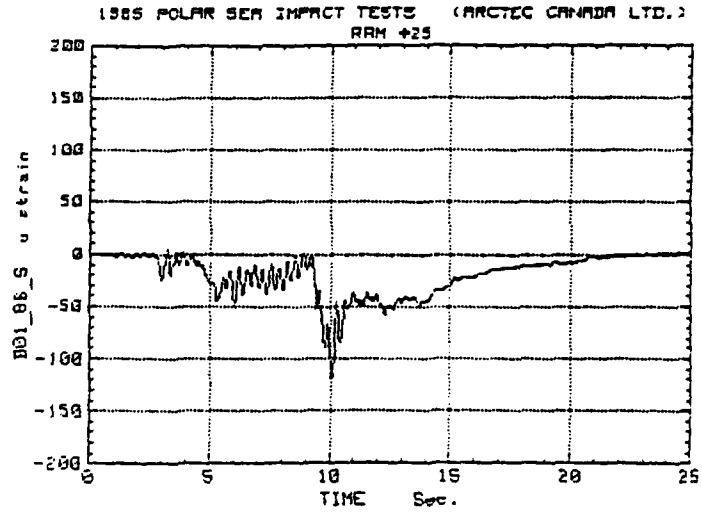

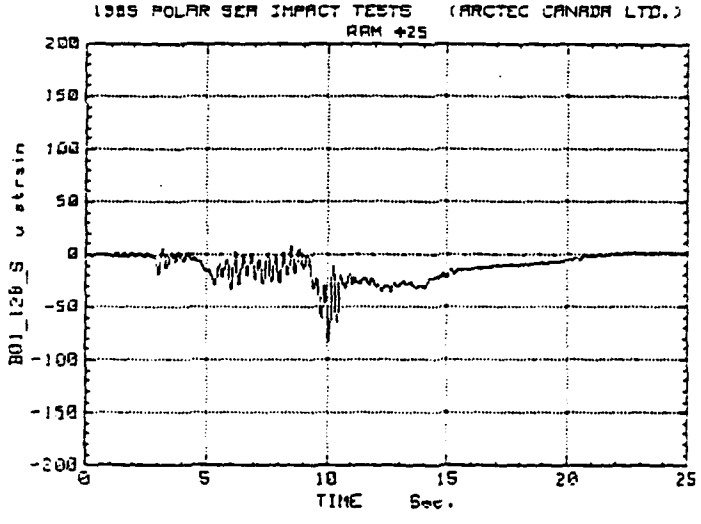

PROGRAM USED: CALC1
ANALYSIS DATE/TIME: 20 Jan 1986/16:50:10
ACQUISTION DATE/TIME: 10 Oct 1985/18:01:55

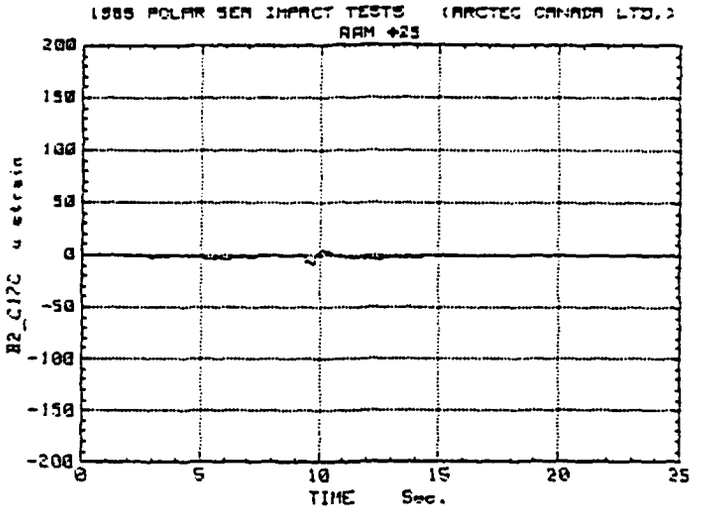

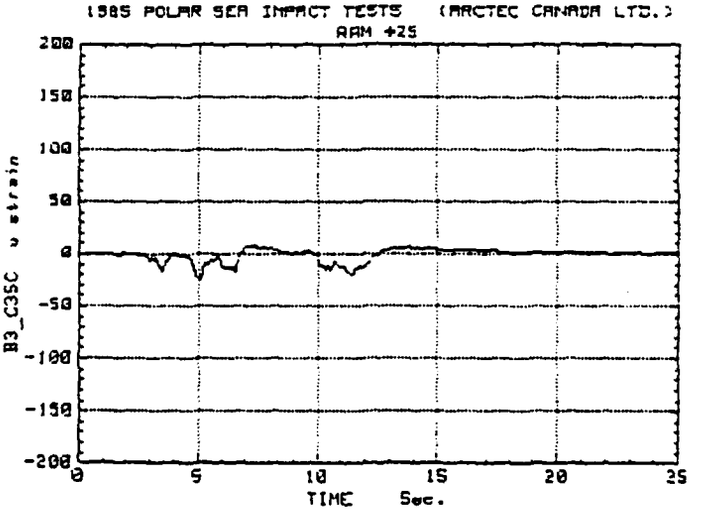

PROGRAM USED: CALC1
ANALYSIS DATE/TIME: 20 Jan 1986/16:51:22
ACQUISTION DATE/TIME: 10 Oct 1985/18:01:55

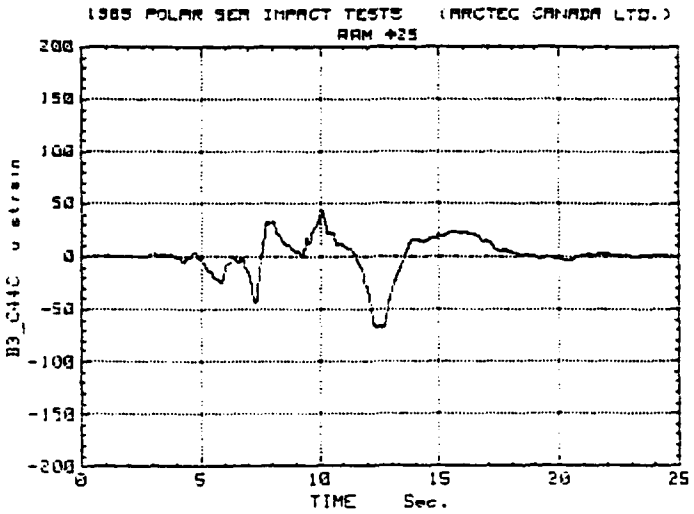

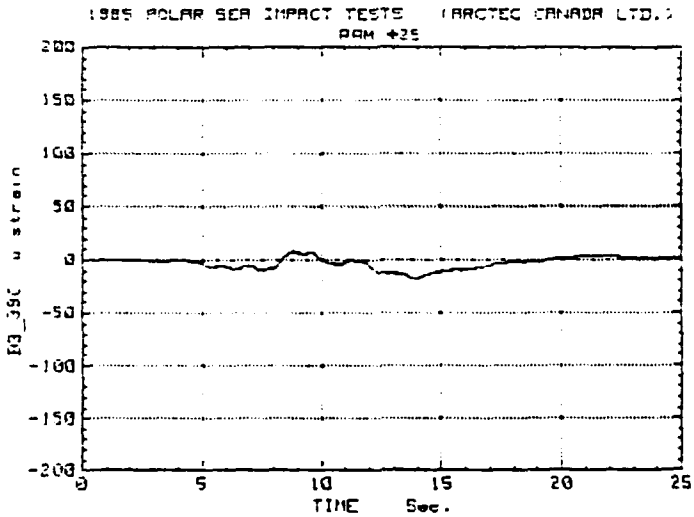

PROGRAM USED: CALC1
ANALYSIS DATE/TIME: 20 Jan 1986/16:52:35
ACQUISTION DATE/TIME: 10 Oct 1985/18:01:55

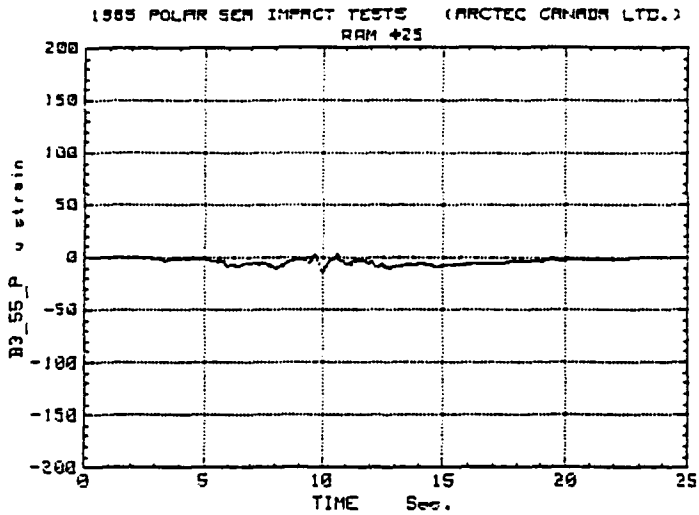

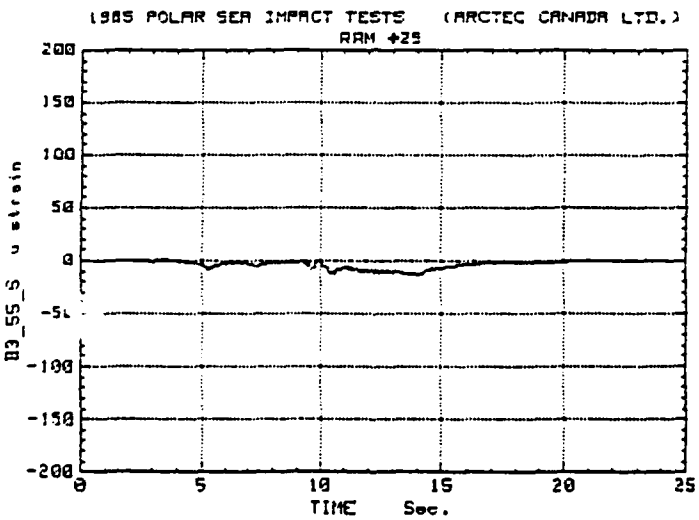

PROGRAM USED: CALC1
ANALYSIS DATE/TIME: 20 Jan 1986/16:53:48
ACQUISTION DATE/TIME: 10 Oct 1985/18:01:55

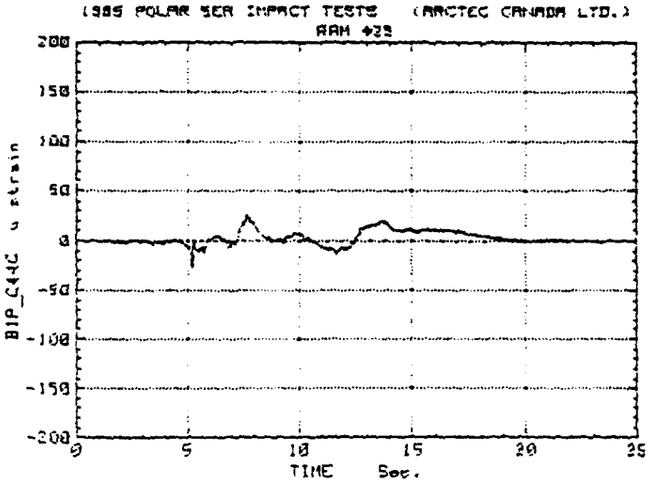

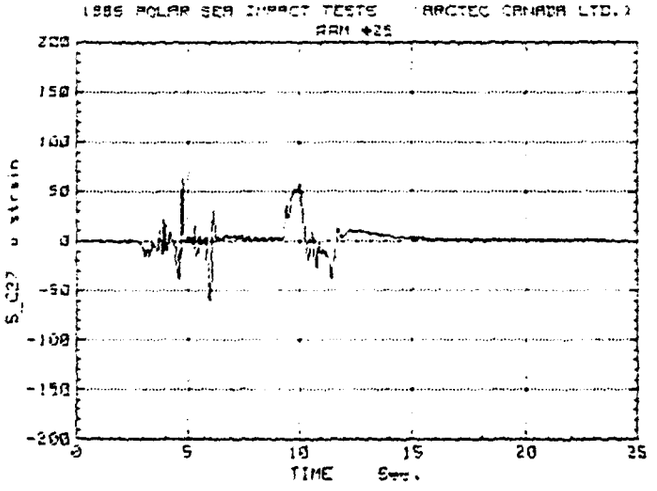

PROGRAM USED: CALC1
ANALYSIS DATE/TIME: 20 Jan 1986/16:55:01
ACQUISITION DATE/TIME: 10 Oct 1985/18:01:55

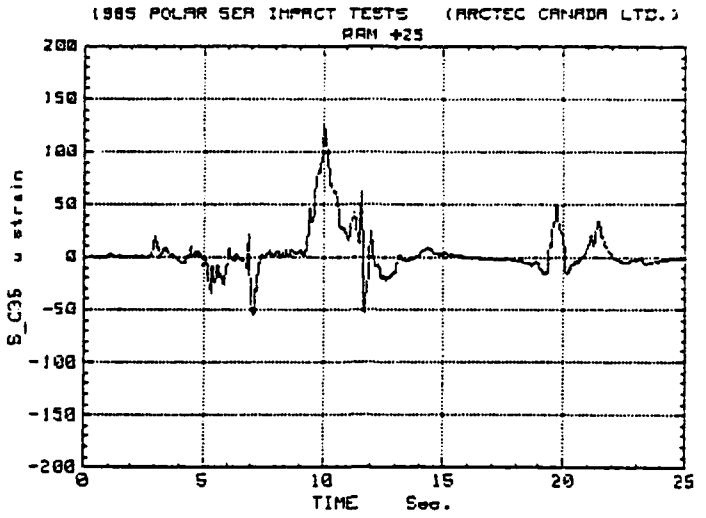

PROGRAM USED: CALC1
ANALYSIS DATE/TIME: 20 Jan 1986/16:55:38
ACQUISTION DATE/TIME: 10 Oct 1985/18:01:55

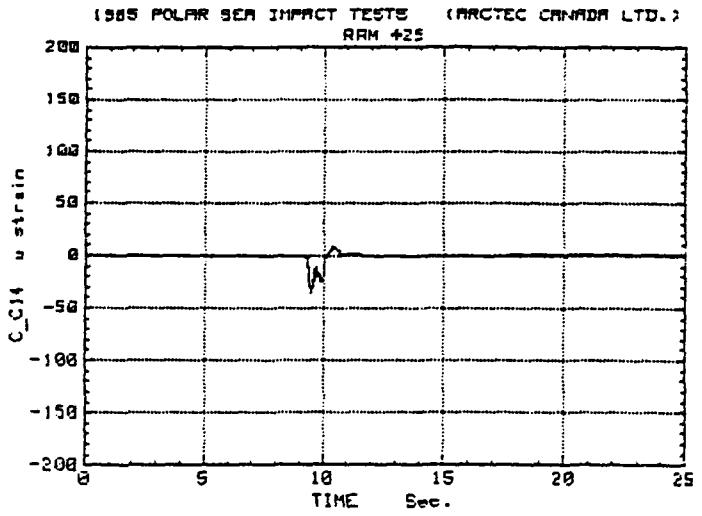

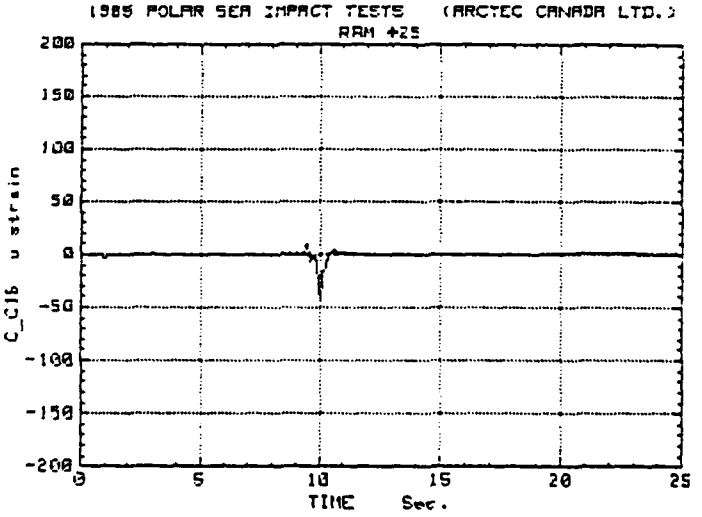

PROGRAM USED: CALC1
ANALYSIS DATE/TIME: 20 Jan 1986/16:56:50
ACQUISTION DATE/TIME: 10 Oct 1985/18:01:55

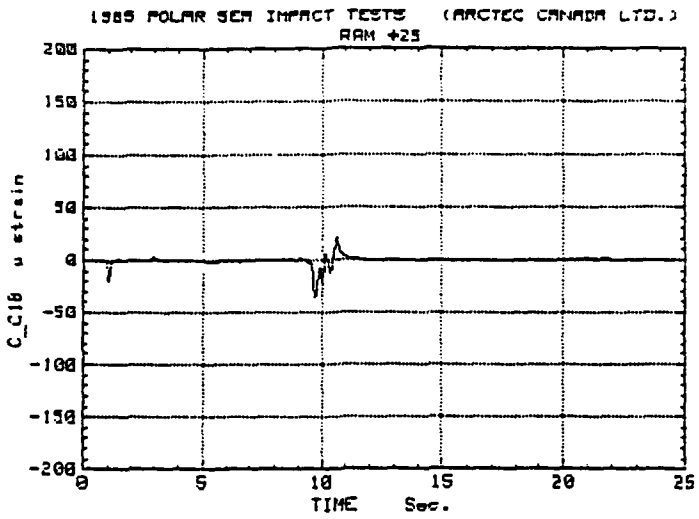

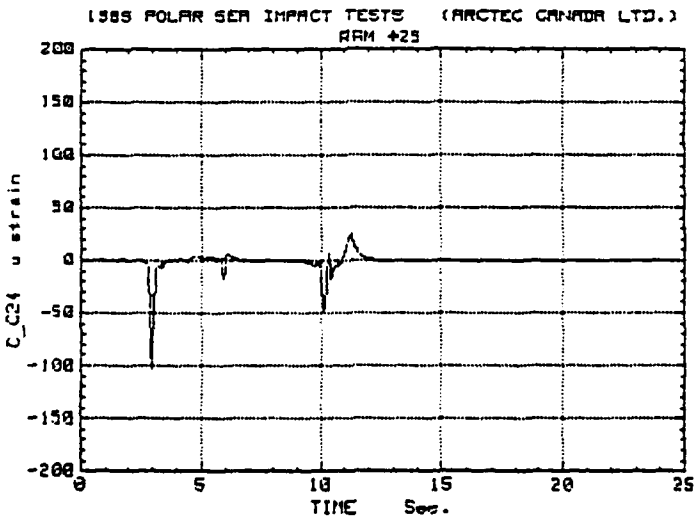

PROGRAM USED: CALC1
ANALYSIS DATE/TIME: 20 Jan 1986/16:58:03
ACQUISTION DATE/TIME: 10 Oct 1985/18:01:55

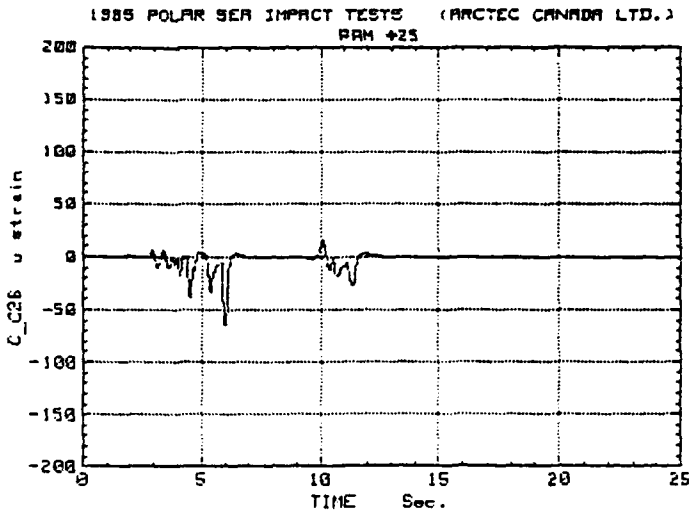

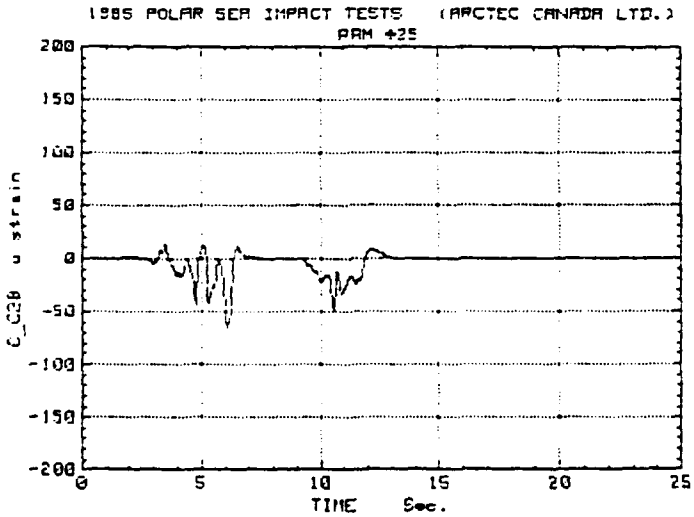

PROGRAM USED: CALC1
ANALYSIS DATE/TIME: 20 Jan 1986/16:59:16
ACQUISTION DATE/TIME: 10 Oct 1985/18:01:55

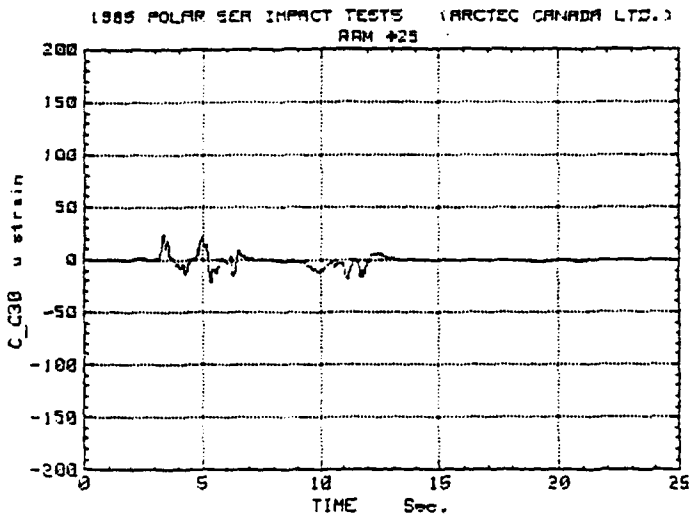

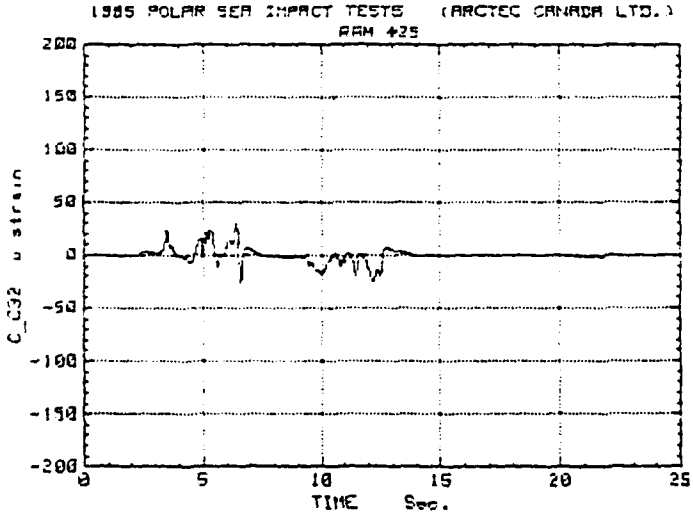

PROGRAM USED: CALC;
ANALYSIS DATE/TIME: 20 Jan 1986/17:00:29
ACQUISTION DATE/TIME: 10 Oct 1985/18:01:55

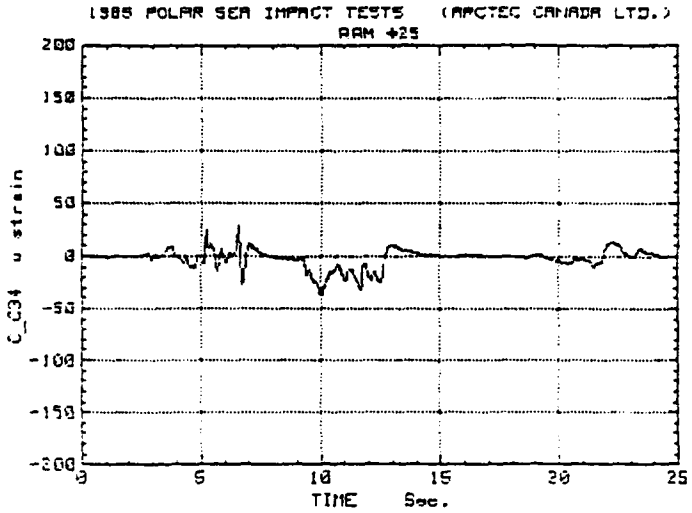

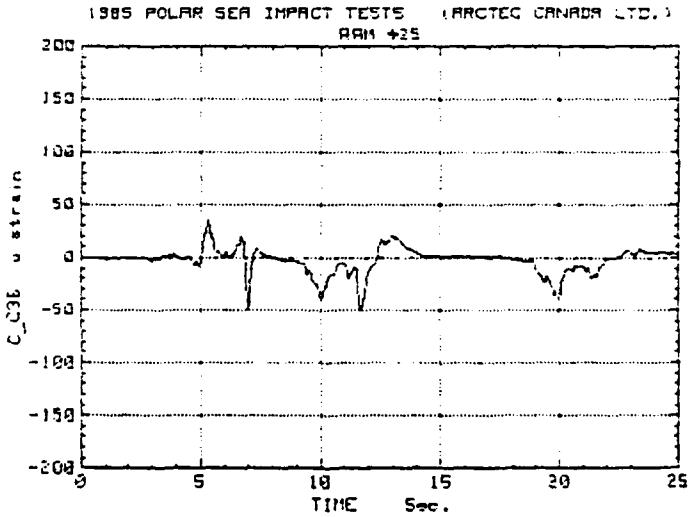

PROGRAM USED: CALC1
ANALYSIS DATE/TIME: 20 Jan 1986/17:01:42
ACQUISTION DATE/TIME: 10 Oct 1985/18:01:55

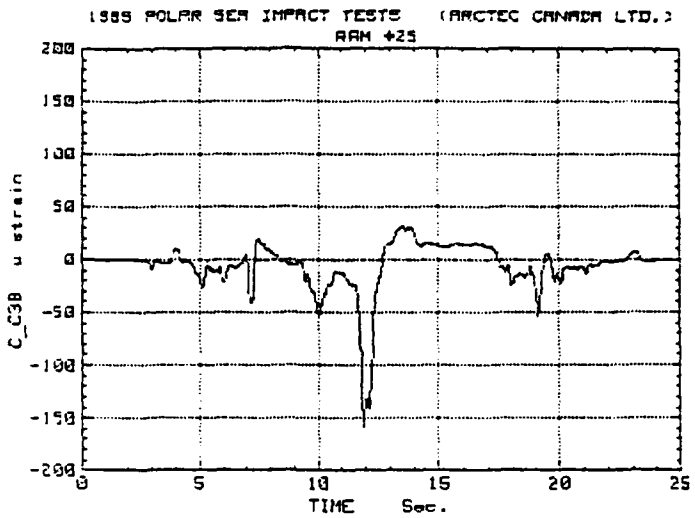

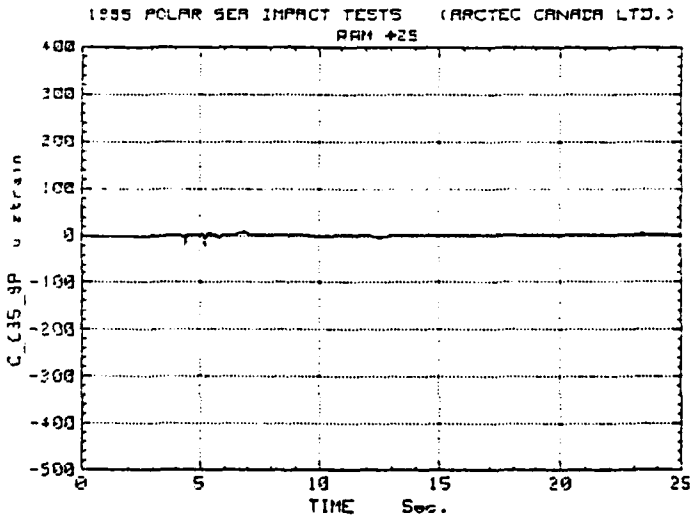

PROGRAM USED: CALC1
ANALYSIS DATE/TIME: 20 Jan 1986/17:02:55
ACQUISTION DATE/TIME: 10 Oct 1985/18:01:55

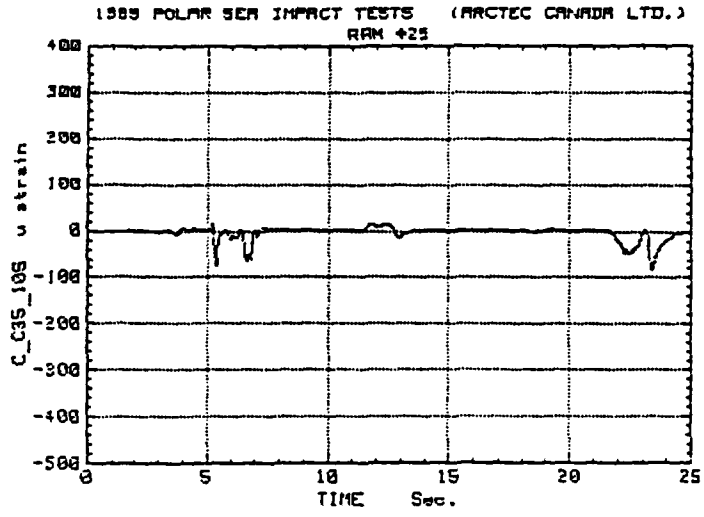

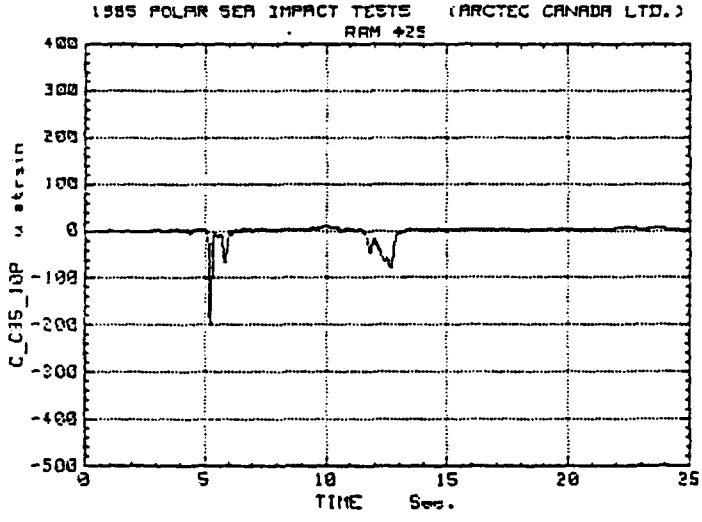

PROGRAM USED: CALC1
ANALYSIS DATE/TIME: 20 Jan 1986/17:04:08
ACQUISTION DATE/TIME: 10 Oct 1985/18:01:55

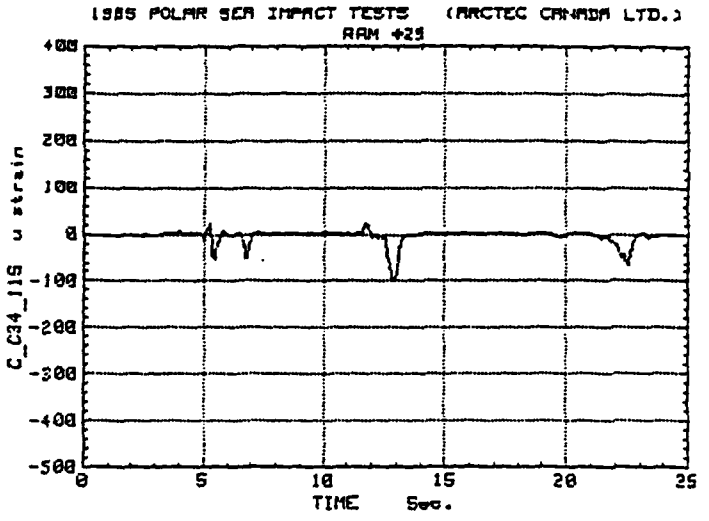

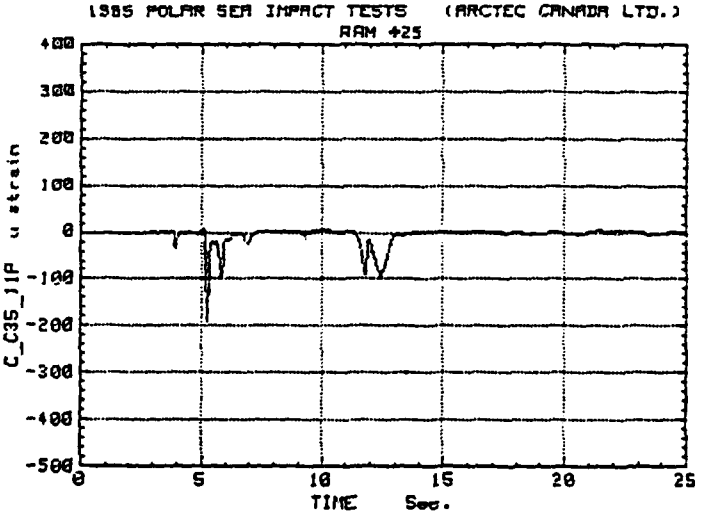

PROGRAM USED: CALC1
ANALYSIS DATE/TIME: 20 Jan 1986/17:05:22
ACQUISTION DATE/TIME: 10 Oct 1985/18:01:55

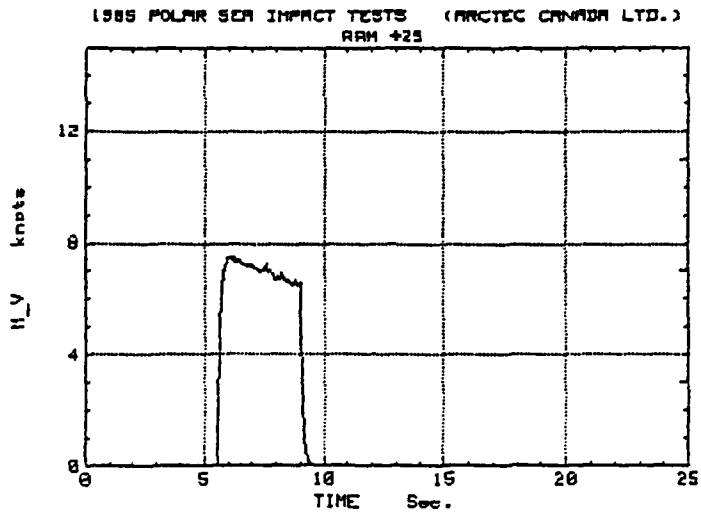

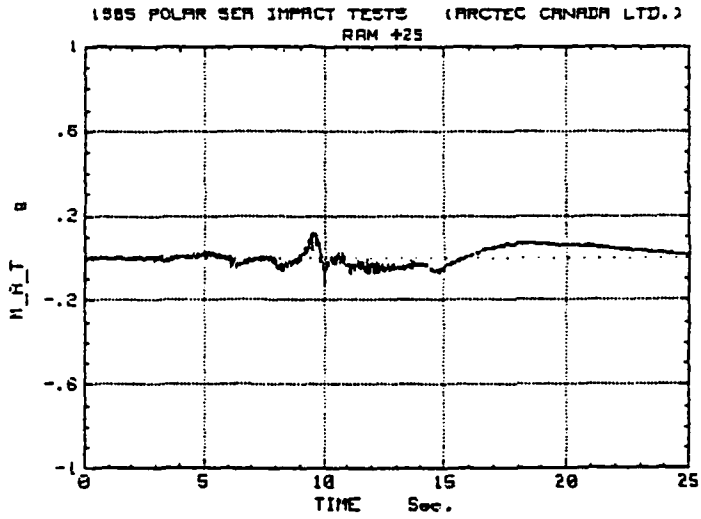

PROGRAM USED: CALC1
ANALYSIS DATE/TIME: 20 Jan 1986/17:06:33
ACQUISTION DATE/TIME: 10 Oct 1985/18:01:55

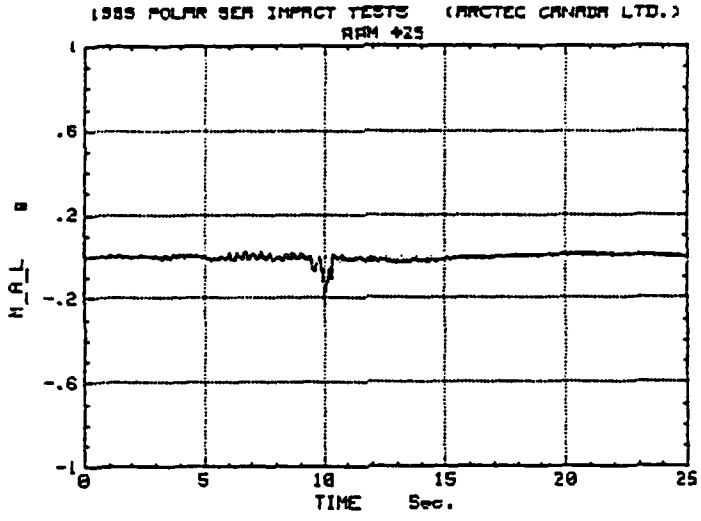

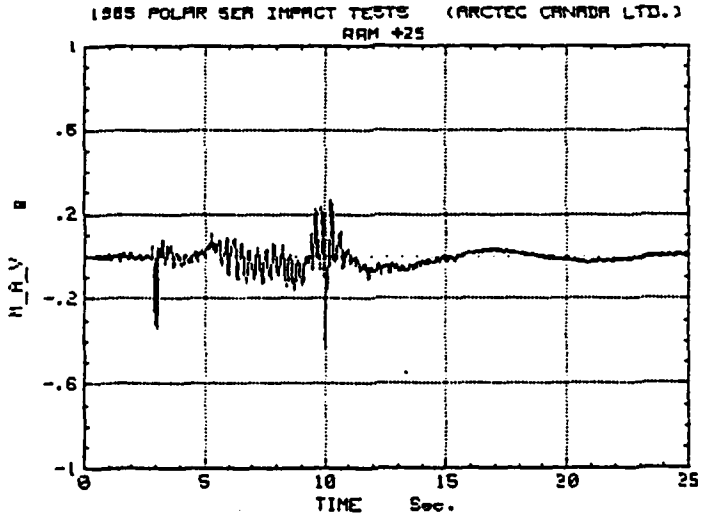

PROGRAM USED: CALC1
ANALYSIS DATE/TIME: 20 Jan 1986/17:07:45
ACQUISTION DATE/TIME: 10 Oct 1985/18:01.55